Onset of Re-epithelialization After Skin Injury Correlates with a Reorganization of Keratin Filaments in Wound Edge Keratinocytes: Defining a Potential Role for Keratin 16

Rudolph D. Paladini, Kenzo Takahashi, Nicola S. Bravo, and Pierre A. Coulombe

Departments of Biological Chemistry and Dermatology, The Johns Hopkins University School of Medicine, Baltimore, Maryland 21205

Abstract. Injury to stratified epithelia causes a strong induction of keratins 6 (K6) and 16 (K16) in post-mitotic keratinocytes located at the wound edge. We show that induction of K6 and K16 occurs within 6 h after injury to human epidermis. Their subsequent accumulation in keratinocytes correlates with the profound reorganization of keratin filaments from a pan-cytoplasmic distribution to one in which filaments are aggregated in a juxtanuclear location, opposite to the direction of cell migration. This filament reorganization coincides with additional cytoarchitectural changes and the onset of re-epithelialization after 18 h post-injury. By following the assembly of K6 and K16 in vitro and in cultured cells, we find that relative to K5 and K14, a well-characterized keratin pair that is constitutively expressed in epidermis, K6 and K16 polymerize into short 10-nm filaments that accumulate near the nucleus, a property arising from K16. Forced expression of human K16 in skin keratinocytes of transgenic mice causes a retraction of keratin filaments from the cell periphery, often in a polarized fashion. These results imply that K16 may not have a primary structural function akin to epidermal keratins. Rather, they suggest that in the context of epidermal wound healing, the function of K16 could be to promote a reorganization of the cytoplasmic array of keratin filaments, an event that precedes the onset of keratinocyte migration into the wound site.

As a typical stratified squamous epithelium, the epidermis shows a polarity in its functional organization and morphology. This polarity reflects the maintenance of an optimal balance between proliferation and differentiation, such that this self-renewing tissue maintains an architecture that is ideal for a barrier function. Progenitor cells reside in the basal layer, where keratinocytes are mitotically active, have a low columnar shape, appear relatively undifferentiated, and express specific markers such as the type II keratin K5 and type I keratins K14 (Nelson and Sun, 1983). Upon commitment to differentiation, basal keratinocytes exit the cell cycle and migrate upward to the suprabasal compartment (Fuchs, 1993). This commitment triggers a specific program of gene expression during which suprabasal keratinocytes steadily progress towards a cytoarchitecture in which they are completely flattened, have lost their organelles and nucleus, and have most of their protein content covalently cross-linked via the action of transglutaminases (Rice and Green, 1979). It is believed that commitment to terminal differentiation, which is accompanied by a switch in keratin gene expression from K5/K14 to K1 (type II) and K10 (type I) (e.g., Fuchs and Green, 1980), is irreversible (Hotchin et al., 1993).

Early studies of the re-epithelialization of full-thickness epidermal wounds in human, mouse, rabbit, dog, and pig skin established that keratinocyte migration and proliferation are initiated at 16–24 h following injury (Winter, 1962; Viziam et al., 1964; Odland and Ross, 1968; Croft and Tarin, 1970; Krawczyk, 1971; Winstanley, 1975; Ortonne et al., 1981; Mansbridge and Knapp, 1987). Cell migration occurs in the form of a stratified epithelial sheet, and in its early phase is unaffected by inhibitors of cell mitosis (e.g., Matoltsy, 1955; see Bereiter-Hahn, 1984). However, a transient burst of enhanced mitotic activity is necessary to supply the cells required to sustain re-epithelialization, and is carried out by a distinct subpopulation of epidermal keratinocytes located behind the migrating epithelium (see Bereiter-Hahn, 1984; Clark, 1993). Ultrastructural studies revealed major cytoarchitectural changes in keratinocytes located at the wound edge, coinciding with the onset of a migratory behavior. These changes include cellular hypertrophy, a fragmentation of keratin filaments and their retraction from the cytoplasmic periphery, and alterations in the number and structure of desmosomes, correlating with the widening of the intercellular space between keratinocytes (e.g., Odland and Ross, 1968; Gabbiani et al.,

Address correspondence to Dr. Pierre A. Coulombe, Department of Biological Chemistry, Johns Hopkins University School of Medicine, 725 N. Wolfe St., Baltimore, MD 21205. Tel.: (410) 614-0510. Fax: (410) 955-5759.

1978; see Bereiter-Hahn, 1984, and Clark, 1993). Taken together, these observations suggest that during the re-epithelialization of skin wounds, epidermal keratinocytes located at the wound edge deviate from their program of terminal differentiation. The cellular and molecular mechanisms responsible for the cytoarchitectural changes, keratinocyte migration, and hyperproliferation after skin injury remain largely unknown.

Keratins, the epithelial-specific intermediate filament proteins, are the major differentiation-specific proteins in epidermis. The >30 known keratin genes and their encoded proteins (40–70 kD MW) are classified as type I (acidic, numbered K9-K20) and type II sequences (basic, numbered K1-K8) (Fuchs and Weber, 1994). Assembly of keratin filaments begins with the formation of a type I-type II coiled-coil heterodimer (see Coulombe, 1993), and this strict requirement calls for the coexpression of at least one type I and one type II keratin gene in epithelial cells. Many keratin genes, such as K5/K14 and K1/K10, are regulated in a differentiation-specific and pairwise fashion (see O'Guin et al., 1990; Fuchs, 1993). In normal epidermis, the function of the keratin filament network is to provide the physical strength that is necessary to maintain cellular integrity in response to a normal load of mechanical stress. In transgenic mice as well as human subjects, mutations or the complete absence of a keratin protein in the epidermis results in defective 10-nm filament structure, mechanical stress-induced cytolysis and blistering (see Fuchs and Coulombe, 1992; Chan et al., 1994; Rugg et al., 1994; Lloyd et al., 1995, and references therein). The location of epidermal tissue cleavage, and thus the cell layer(s) affected by trauma, are determined by the pattern of expression of the mutation-bearing keratin. Mutations affecting specific keratin genes underlie several inheritable skin blistering disorders such as epidermolysis bullosa simplex, epidermolytic hyperkeratosis, and palmoplantar keratoderma (see Coulombe, 1993; Fuchs et al., 1994; McLean and Lane, 1995).

Injury to the skin significantly alters keratin gene expression in keratinocytes located near the wound edge. Under such conditions, an induction of K6 (type II), K16 and K17 (type I) occurs in the differentiating layers of epidermis (e.g., Weiss et al., 1984; O'Guin et al., 1990). K6 and K16 proteins have been biochemically detected at 8–10 h in the wounded tissue (Tyner and Fuchs, 1986; Mansbridge and Knapp, 1987; de Mare et al., 1990). Subsequent to this induction, the differentiation-specific keratins K1 and K10 appear down-regulated (e.g., Mansbridge and Knapp, 1987; Coulombe et al., 1991). In addition to wound healing in skin, K6 and K16 are also expressed in stratified epithelia undergoing chronic hyperproliferation or abnormal differentiation, including cancer (Moll et al., 1983; Weiss et al., 1984; Stoler et al., 1988; Schermer et al., 1989). In such hyperproliferative disorders, as in regenerating stratified epithelia, abundant expression of K6 and K16 is often associated with alterations in keratinocyte differentiation. Consistent with this, overexpression of a wild-type human K16 gene in transgenic mice causes the reorganization of the IF network in keratinocytes of the hair follicle outer root sheath and epidermis, leading to aberrant keratinization and hyperproliferation in these tissues (Takahashi et al., 1994). Yet, K6 and K16 are constitutively expressed in a variety of epithelial tissues under normal conditions (e.g., Moll et al., 1982, 1983), without apparent consequences for their differentiation. Thus, the role(s) that K6 and K16 may play during wound healing, as well as the consequences of their expression in chronic hyperproliferative diseases affecting stratified epithelia, remain unclear.

We investigated the consequences of K6 and K16 induction in keratinocytes located at the wound edge after injury to epidermis. We characterized the time-course of K6 and K16 induction in wounded human skin, and correlated it with alterations in keratinocyte cytoarchitecture. We found that induction of K6 and K16 proteins occurs within 6 h at the wound edge, and that their subsequent accumulation correlates with a polarized reorganization of keratin filaments in suprabasal keratinocytes, followed by alterations in their shape and cell–cell adhesion. These changes coincide with the onset of re-epithelialization, which begins after 18 h post-injury. To determine whether K6 and K16 could play a direct role in these phenomena, we investigated their assembly properties in vitro as well as in vivo. We show that unlike K5, K6, and K14, human K16 features unusual assembly properties, in that it promotes the formation of short 10-nm filaments that are localized preferentially near the nucleus in transfected cells as well as in skin keratinocytes of transgenic mice. Our data suggest that the alterations in keratin expression, and in particular the induction of K16, could play a role in promoting the reorganization of keratin filaments that occurs in spinous keratinocytes before the onset of re-epithelialization after injury to epidermis.

Materials and Methods

Human Skin Wound Healing Studies

Studies involving human subjects were reviewed and approved by the Joint Committee on Clinical Investigation at the Johns Hopkins University School of Medicine. All experiments were performed under sterile conditions. Small incisions (6 mm long, 2 mm deep) were made on the inside arm of healthy volunteers (26–35 years of age). This site was selected because of the unusually low density of hair follicles. For sampling, 4-mm punch biopsies (Acu-Punch; Acuderm Inc., Ft. Lauderdale, FL) were performed under local anesthesia at either 6, 12, 18, or 30 h after wounding. Each biopsy was divided into two pieces across the wound: one-third of the sample was processed for routine electron microscopy (Coulombe et al., 1989) while the remaining two-thirds was embedded in TBS tissue freezing medium (Triangle Biomedical Sciences, Durham, NC), frozen in liquid nitrogen, and stored at −20°C until further processing. For electron microscopy, large size samples (1 mm × 2 mm) were embedded in epoxy resin (Coulombe et al., 1989) to optimize orientation. After curing, the blocks were trimmed (0.5 mm^2) so as to obtain thin sections from wound edge tissue. For indirect immunofluorescence, 5-μm-thick sections were made from the same (frozen) biopsies, without further trimming, so that skin tissue extended ~1.5 mm laterally from the wound site. The primary antibodies used for immunostaining included rabbit polyclonal antisera directed against human K16 (Takahashi et al., 1994), K6 (Stoler et al., 1988), and filaggrin (Dale et al., 1985); a guinea pig polyclonal antisera directed against human K5 (Lersch et al., 1989); and mouse monoclonal antibodies directed against human K17 and K10/K11 (Sigma Chem. Co., St. Louis, MO). Bound primary antibodies were revealed using goat secondary antibodies conjugated to FITC or rhodamine (KPL Laboratories Inc.). Nonwounded skin tissue was used as a control in these experiments.

Production of Human Recombinant K6b and K16

cDNAs encoding K6b and K16 were cloned by applying a coupled reverse transcription-polymerase chain reaction (RT-PCR) as previously reported

(Paladini et al., 1995; Takahashi et al., 1995). Oligonucleotides primers were designed from the published sequences of the human K6b (Tyner et al., 1985) and K16 (Rosenberg et al., 1988) genes and applied on total RNA isolated from cultured primary human epidermal keratinocytes. To facilitate the subcloning of the cDNA clones into either plasmid pET-8c (Studier et al., 1990) or pGEM5zf (Promega Corp., Madison, WI), each primer had a 10-nt extension on its 5′ end that contained a restriction enzyme recognition sequence. Recombinant clones were grown, and the entire cDNA inserts subjected to sequencing. The amino acid sequence predicted from the K6b cDNA clone selected corresponds to that of the previously cloned gene (see Takahashi et al., 1995). In the K16 cDNA clone, the first codon was altered (Thr→Ala) as a result of the subcloning strategy (see Paladini et al., 1995). An identical change in the human K14 cDNA was shown to have no apparent effect on its assembly behavior in vitro (Coulombe and Fuchs, 1990).

Keratin Expression, Purification, and Immunological Analyses

We used an *Escherichia coli* expression system based on the phage T7 RNA polymerase gene (Studier et al., 1990) to generate mg quantities of recombinant human epidermal keratins as described (Coulombe and Fuchs, 1990). Plasmids pET-K5 and pET-K14 (Coulombe and Fuchs, 1990), as well as pET-K6b and pET-K16 (this study) were individually transformed into *E. coli* strain BL21 (DE3), grown to OD_{600} of ~0.5, and recombinant keratin expression was induced by adding isopropyl-β-D-thiogalactopyranoside to 1 mM and carried out for 5 h. Inclusion bodies were isolated from lysed bacterial pellets and solubilized in a buffer containing 6.5 M urea, 50 mM Tris-HCl, 2 mM DTT, 1 mM EGTA, 1 mM PMSF, pH 8.1 (Q buffer). Recombinant keratins were purified to near-homogeneity by chromatography in Q buffer on a Pharmacia FPLC Mono Q anion-exchange column operated at 0.5 ml·min^{-1}. Proteins of interest were eluted with a 0–200 mM linear gradient of guanidine-HCl over a 15-ml vol, and 0.5-ml fractions were collected and analyzed by 10% SDS-PAGE. Native human keratins were isolated from cultured SCC-13 cells, a squamous skin carcinoma cell line (Wu et al., 1982), using the high-salt extraction method (Lowthert et al., 1995). The final pellet was solubilized in Q buffer, and subjected to Mono Q chromatography as described above. Protein concentration was determined by the Bradford assay (Bradford, 1976) using reagents purchased from Bio-Rad Labs. (Richmond, CA). For immunoblot analyses, known quantities of recombinant and native human keratins were electrophoresed, electroblotted to nitrocellulose, and the blots incubated with diluted primary antisera prepared in blocking buffer (Tris-buffered saline with 0.5% Tween 20 and 5% dry milk). Bound primary antibodies were revealed by alkaline phosphatase-conjugated secondary antibodies as recommended by the manufacturer (Bio-Rad Labs.).

Chemical Cross-Linking

Mono Q fractions containing heterotypic keratin complexes were used for chemical cross-linking as previously described (Coulombe and Fuchs, 1990). Purified recombinant type I and type II keratins were mixed in a ~45:55 molar ratio at a final concentration of 750 μg·ml^{-1} and resubjected to the anion-exchange chromatography protocol described above. Mono Q fractions containing heterotypic complexes were dialyzed overnight against 25 mM sodium phosphate, 10 mM β-ME, containing either 6.5 or 8 M urea at pH 7.4, to remove Tris ions, which interfere with the cross-linking agents. Protein concentration was adjusted to 200 μg·ml^{-1}. Chemical cross-linking was performed by adding BS3 (bis-(sulfosuccinimidyl) suberate; 10 mM) for 1 h at 12°C (Geisler et al., 1992). In some experiments, glutaraldehyde was used at similar concentrations (see Coulombe and Fuchs, 1990). Cross-linked products (3 μg total protein) were resolved on a 3–17.5% gradient SDS-PAGE, and stained with Coomassie blue. The apparent molecular mass of cross-linked species was calculated from a standard curve established with proteins of known molecular mass values.

In Vitro Keratin Filament Assembly, Negative Staining, and Electron Microscopy

Mono Q fractions containing heterotypic keratin complexes were used for in vitro polymerization assays as previously described (Coulombe and Fuchs, 1990). Polymerization was achieved by extensive dialysis of 0.25-ml samples at 200 μg·ml^{-1} against 5 mM Tris-HCl, 10 mM β-ME, pH 7.4. Dialysis was carried out at 4°C for 16–24 h for optimal results. In some experiments, the polymerization buffer was modified in terms of its ionic strength (50 mM Tris-HCl), pH (7.0), and presence of salt (150 mM NaCl). Polymerized keratins were adsorbed onto glow-discharged carbon-coated 400 mesh grids (Ted Pella Inc., Redding, CA), negatively stained with 1% aqueous uranyl acetate/0.025% tylose, and visualized on a Zeiss EM10A electron microscope operated at 60 kV. Micrographs were recorded at a nominal magnification of 31,500×, and the magnification was calibrated using a carbon grating replica (Ernest Fullam no. 10021). For filament width determination, micrographs were printed (magnification: 120,000×) and a total of 60 filaments were sampled for each type I-type II combination considered in this study (10 randomly sampled filaments per each of three micrographs for each of two distinct assembly experiments). For the determination of polymerization efficiency, final assemblies (80-ul aliquots, corresponding to ~20 ug proteins) were centrifuged at 100,000 *g* for 40 min at 4°C, and supernatant and pellet fractions were analyzed by SDS-PAGE, Coomassie-blue staining, and gel scanning densitometry (MCID; Imaging Research Inc.).

Transient Expression of Keratin cDNAs in Cultured Cells In Vitro

Keratin cDNAs were subcloned from pET vectors into the GW1-CMV expression plasmid, featuring a cytomegalovirus promoter and a SV-40 polyadenylation signal. In the case of K16, an 11-kb genomic DNA fragment containing the entire functional gene (Rosenberg et al., 1988) was also subcloned in this expression vector. Transient transfection assays were performed in BHK-21 cells, a hamster kidney cell line (see Quinlan and Franke, 1982), and in PtK2 cells, a rat kangaroo kidney epithelial cell line (Franke et al., 1978). All transfections were done on subconfluent cells grown on 22-mm^2 glass coverslips using the calcium phosphate precipitation method (see Letai et al., 1992). At 24, 36, 48, or 72 h posttransfection, cells were fixed with absolute methanol for 20 min at −20°C and processed for morphological analysis. For indirect double-immunofluorescence studies, transfected keratins were detected with combinations of the primary and secondary antibodies described above. In addition, we used the mouse monoclonal antibody L2A1, which recognizes K8-K18 complexes (Chou et al., 1993), and the V9 Mouse monoclonal antibody directed against vimentin (Sigma Chem. Co.). As routine controls in all labeling protocols, mock-transfected cells were processed in parallel with the relevant antisera.

Quantitation of Epidermal Keratins in Transfected PtK2 Cells

PtK2 cells were seeded on 100-mm plates that contained one 22-mm^2 glass coverslip. A plate was transfected with either control CMV plasmid, CMV-K14 cDNA, or CMV-K16 cDNA exactly as described above. The amounts of DNA and the volume of calcium phosphate precipitates were scaled up on a per surface area basis to maintain conditions similar to those used for the experiments described above. At 72 h posttransfection, the glass coverslip was removed and processed for immunofluorescence staining to determine transfection efficiency. The remaining cells on the 100-mm dish were recovered by scraping and a Triton X-100/high salt insoluble extract was prepared as described (Lowthert et al., 1995). The final pellets were solubilized in Q buffer and protein concentrations determined as described above. For SDS-PAGE/immunoblot analyses, known amounts of purified recombinant K14 or K16 (5 ng; 10 ng; 25 ng; 50 ng) were coelectrophoresed with 1.5 μg of extracts prepared from transfected cells (control CMV, K14, and K16), and blotted onto nitrocellulose. Blots were incubated with the polyclonal anti-K14 or anti-K16 antiserum, and bound primary antibodies were revealed by enhanced chemiluminescence as per the manufacturer's instructions (Amersham Corp., Arlington Heights, IL). To allow for a direct comparison of the K14 and K16 blots, the primary antibody dilutions were adjusted in preliminary experiments using serially diluted keratin standards.

Results

The Accumulation of K6, K16, and K17 at the Wound Edge Correlates with Changes in Keratinocyte Cytoarchitecture

We examined the temporal and spatial relationships be-

tween the induction of K6, K16, and K17 expression and the onset of re-epithelialization after full epidermal thickness injury to the skin of four healthy volunteers. Our sampling strategy covered the initial 30 h after injury, based on data available from previous studies (see Introduction). Samples were obtained at 6, 12, 18, and 30 h after wounding, and analyzed by light and electron microscopy as well as indirect immunofluorescence. The antigens localized included keratins K5, K6, K16, K17, and K10, and filaggrin, a keratin filament-aggregating activity that is expressed late during terminal differentiation (Dale et al., 1985). Due to the limited number of human skin biopsies available, we restricted our electron microscopy analyses to the proximal portion of the wound edge, while the frozen sections prepared from the same biopsies typically extended ~1.5 mm laterally from the wound site. Collectively these data allowed us to monitor changes in keratin synthesis, keratinocyte differentiation and migration, cell shape, and cell–cell adhesion at the wound edge.

The earliest time at which significant morphological changes were detected in epidermis at the wound edge was 18 h after injury. The epidermis proximal to the wound edge was slightly thickened and disorganized compared to earlier time points (Fig. 1, *A* and *B*). Epidermal thickening appeared to result from cytoarchitectural changes in suprabasal keratinocytes, since many showed an altered shape (see below) while no significant increase in mitotic activity was detectable in epidermis at 18 h (not shown). Ultrastructural analysis showed that in many spinous layer keratinocytes, keratin filament bundles were reorganized and often aggregated, leaving large portions of cytoplasm relatively depleted of filaments (Fig. 1, compare *D* and *E*). As reported previously (e.g., Odland and Ross, 1968; Winstanley, 1975), many spinous keratinocytes featured membrane-bound vacuoles in their cytoplasm (Fig. 1 *E*), and the intercellular spaces were considerably enlarged. At 30 h post-injury, these alterations were more pronounced and extended further away from the edge, and re-epithelialization of the wound site was clearly under way, in the form of a stratified epithelium (Fig. 1 *C*). Many spinous keratinocytes near the wound edge and in the migrating tongue showed an enlarged size and elongated shape with their keratin filaments aggregated near the nucleus, on the side opposite to the wound site (Fig. 1 *F*). These elongated spinous keratinocytes were more frequent at 30 h compared to 18 h after injury, and were clearly oriented towards the wound site, suggestive of a migratory activity. Although basal keratinocytes also featured significant changes (see Coulombe et al., 1991), the acquisition of an elongated and polarized morphology was specific to spinous layer keratinocytes. Additional ultrastructural changes seen in spinous keratinocytes near the wound site at 18 and 30 h after injury included a reduction in the number of desmosomes, and the occurrence of thin cytoplasmic processes at the cell surface (Fig. 1, *E* and *F*). The timing and nature of these alterations at the epidermal wound edge are very similar to what has been reported previously (Odland and Ross, 1968; Krawczyk, 1971; Winstanley, 1975).

Immunofluorescence staining of fresh frozen sections prepared from these wound samples showed that significant amounts of K6 and K16 proteins are present in suprabasal keratinocytes at the wound edge as early as 6 h after injury (compare K16 stainings in Fig. 2, *A* and *B*). It is noteworthy that occasional spinous keratinocytes showed a K16 signal in intact human epidermis (Fig. 2 *A*), although this signal was comparatively weak compared to cross-sectioned sweat gland ducts profiles (which also contain K16; Moll et al., 1983)[1]. The signal for both keratins was much stronger by 12 h (Fig. 2 *C*, K16 staining) and especially by 18 h post-injury (Fig. 2 *D*, K16 staining). Interestingly, the K16 signal extended throughout the suprabasal layers of epidermis proximal to the wound edge, where the tissue shows thickening, whereas away from the wound edge, where the tissue is of normal thickness, it appeared restricted to the first layer of suprabasal cells (e. g., Fig. 2 *C*). A signal for K17 was first detected in 12-h samples, and became prominent by 18 h, especially in the uppermost layers of the epidermis proximal to the wound edge (Fig. 2 *E*). By 30 h, the K17 signal was stronger, but remained more restricted to the wound edge compared to K16 (Fig. 2, compare *F* with *G*). At 30 h post-injury, an advancing tongue of migrating keratinocytes could be easily recognized (Figs. 1 *C*, 2, *F* and *G*), and most basal cells at the leading edge and in direct contact with the extracellular matrix were positive for the K16, K17 and K10 antigen

1. On immunoblots, the anti-human K16 antiserum used reacts with a single antigen in an IF extract prepared from human foot sole skin. This 48-kD antigen comigrates with purified human recombinant K16 (data not shown). The possibility that K16 could be "constitutively" expressed at very low levels in epidermal keratinocytes will be addressed elsewhere.

Figure 1. Morphological alterations in keratinocytes at the wound edge after injury to human epidermis. Human skin subjected to wounding via scalpel incisions was sampled at either 6, 12, 18, or 30 h post-injury and processed for routine electron microscopy (see Materials and Methods). (*A–C*) Light micrographs of thick sections (0.7 um thick) stained with toluidine blue. The position of the wound edge (*WE*) is indicated. In the 18 h (*B*) and 30 h (*C*) samples, the epidermis proximal to the wound edge is thickened, and the intercellular spaces between keratinocytes are widened. Such changes are not present at the wound edge after 6 h (*A*) or 12 h (not shown). Note as well that re-epithelialization is obvious only in the 30 h sample (*C*, *arrow*). *DE*, dermis; *BA*, basal layer; *SP*, spinous layer; *GR*, granular layer; *SC*, stratum corneum layer. (*D–F*) Electron micrographs of thin sections (50 nm) prepared from the same tissue blocks as *A–C* and stained with uranyl acetate and lead citrate. *D* shows a spinous keratinocyte at the wound edge in the 6-h sample. Its cytoarchitecture is typical of normal epidermis, with a polygonal shape, a centrally located nucleus (*N*), a well-dispersed array of thick keratin filament bundles (*kf*), and numerous desmosomes at the cell surface (*arrows*). *E* shows a spinous keratinocyte at the wound edge in the 18-h sample. This cell is enlarged, and makes few desmosomal contacts (*arrows*) in the context of widened intercellular spaces (*IS*). In particular, keratin filaments (*kf*) are aggregated on one side of the cell, leaving large areas of cytoplasm relatively depleted of filaments (*asterisks*). Many vacuoles (*v*) are seen in the cytoplasm. These cytoarchitectural changes in spinous keratinocytes are more developed and extend further away from the edge in the 30-h sample (*F*). This low-magnification view shows three hypertrophied and elongated spinous keratinocytes featuring a polarized cytoarchitecture with a cytoplasmic projection extending in the direction of the wound site (*double arrows*), and aggregated keratin filaments (*ka*) located on the opposite pole of the cell, near the nucleus (*N*). These keratinocytes appear to be moving towards the wound site. Bars: (*A–C*) 100 μm; (*D*) 2 μm; (*E*) 2.8 μm; (*F*) 4.1 μm.

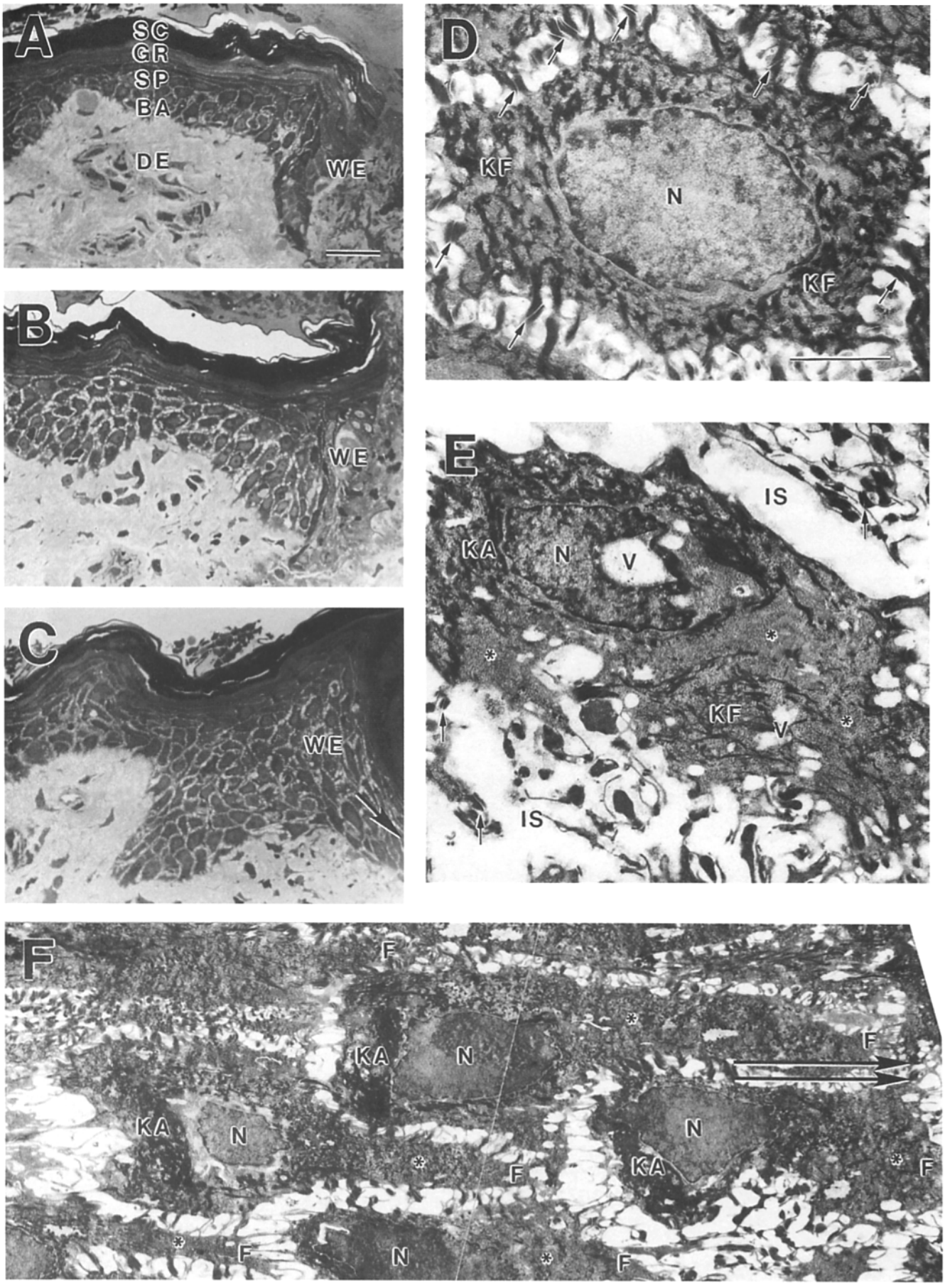
A
SC
GR
SP
BA
DE
WE
B
WE
C
WE
D
KF
N
KF
E
IS
KA
N
V
KF
V
IS
F
F
KA
N
F
KA
N
N
KA
F
F
F
N
F

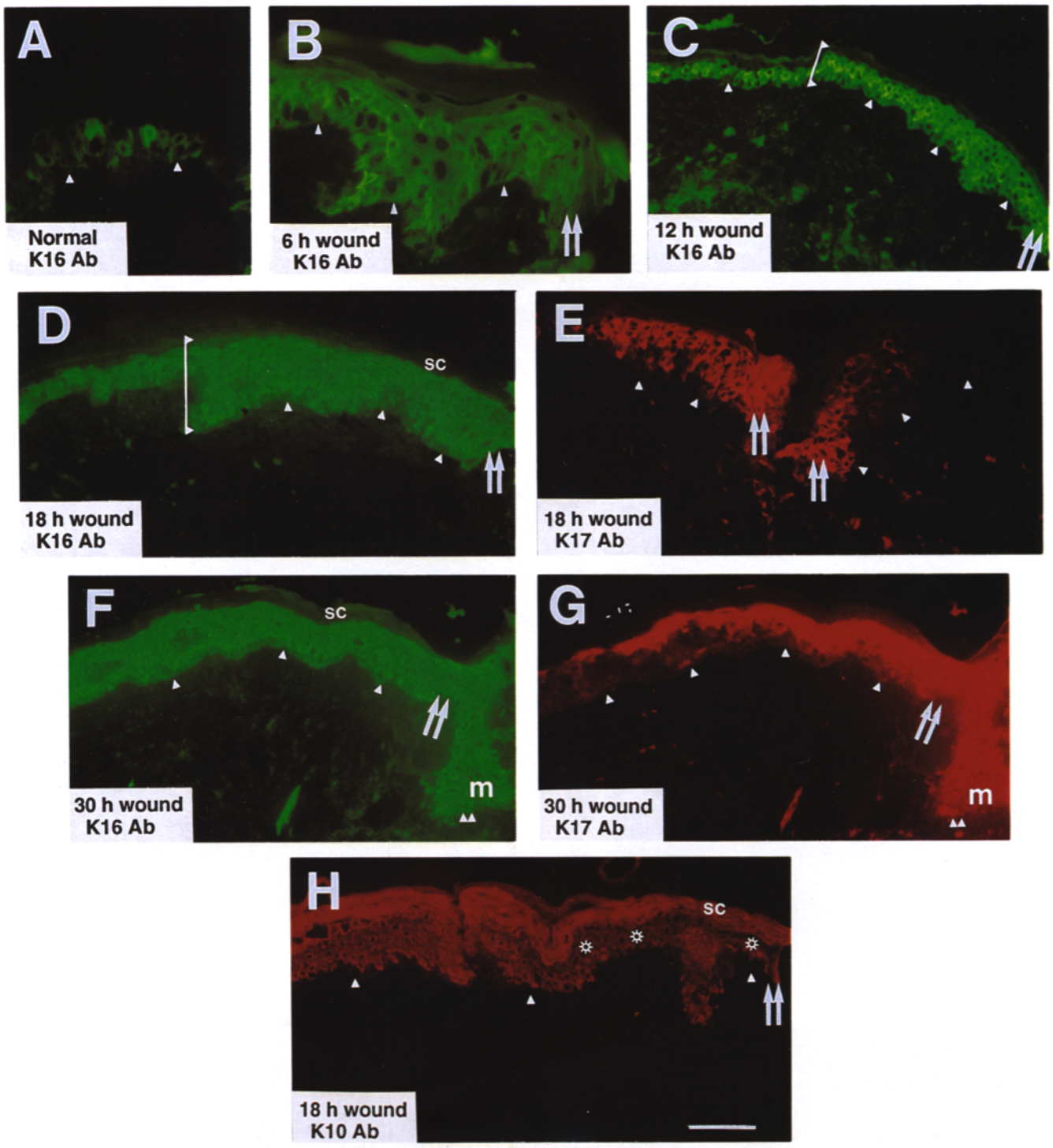

Figure 2. Immunolocalization of biochemical markers at the wound edge after injury to human epidermis. Human skin subjected to wounding via scalpel incisions was sampled at either 6, 12, 18, or 30 h post-injury and processed for frozen sectioning and indirect immunofluorescence (see Materials and Methods). (*A–D* and *F*) K16 stainings in intact human epidermis (*A*), and at the wound edge at 6 h (*B*), 12 h (*C*), 18 h (*D*) and 30 h (*F*). The wound edge is depicted with a set of double arrows, and the position of the dermo-epidermal interface is indicated with arrowheads at several locations. In intact epidermis (*A*), sweat gland ductal epithelium is strongly stained for K16 (not shown), while occasional spinous keratinocytes show faint staining. An induction of K16 in spinous keratinocytes at the wound edge is already apparent at 6 h after epidermal injury (*B*). At later time points, the K16 signal extends in the vertical as well as the horizontal axes (*C* and *D*). Note the vertical extension of the K16 signal proximal to the wound edge correlates with a local thickening of the epidermis, depicted with the brackets on *C* and *D*. (*E* and *G*) K17 stainings at 18 h (*E*) and 30 h (*G*) (note that *F* and *G* represent a double-staining experiment for K16 and K17, respectively). A signal for K17 appears significantly later than K16 and remains more proximal to the wound edge, even at 30 h post-injury (compare *F* and *G*). Note as well that in the migrating tongue of epithelium (*m*) seen in the 30 h samples, a strong signal for K16 and K17 is seen in basal cells (double arrowheads in *F* and *G*). Frame H, K10 staining in the 18 h sample. The signal in the spinous layer is reduced near the wound edge (*asterisks*) compared to the periphery of the sample (*single asterisk*). The stratum corneum layer (*sc*), does not show a reduced K10 staining at the wound edge. Bar: (*A* and *B*) 50 μm; (*C–H*) 100 μm.

(Fig. 2, *F* and *G*). This observation has important implications for the cellular mechanisms of re-epithelialization following full-thickness injury to the epidermis, as discussed below. Localization of additional antigens extended the ultrastructural data demonstrating the occurrence of morphological changes in epidermis proximal to the wound site. At 18 and especially at 30 h, the signal for K5 was fainter in the basal layer and extended into the suprabasal layers, contrasting with its basal-restricted distribution in normal epidermis (not shown). K10, considered as an early marker of differentiation, was still present throughout the suprabasal epidermis, although reduced in intensity in spinous keratinocytes proximal to the wound edge (Fig. 2 *H*). The signal for filaggrin, a late differentiation marker normally present in the granular layer, appeared unchanged in its distribution and intensity at the wound edge (data not shown). Along with the electron microscopy data, this suggests that up to 30 h after injury, there are no significant changes in the uppermost portion of the epidermis.

The results of our examination of the early phase of the response of human epidermis to full-thickness injury are consistent with previous studies involving comparable wounds in human skin (e.g., Odland and Ross, 1968; Krawczyk, 1971). The onset of keratinocyte migration takes place after 18 h and coincides with significant morphological changes in keratinocytes located in the innermost half of epidermis at the wound edge. Our immunostaining data show that K6 and K16 proteins are present at the wound edge as early as 6 h after injury, and are initially detected in lower spinous layer of epidermis. A subsequent accumulation of K6 and K16 in these keratinocytes precedes the onset of cytoarchitectural alterations and migratory behavior. Relative to K6 and K16, the induction of K17 occurs later, and is restricted to the proximal wound edge. Collectively these results suggest that K6, K16, and K17, along with the alterations in the levels of other keratins (e.g., K5/K14; K1/K10), may play a direct role in eliciting the morphological alterations that coincide with the onset of re-epithelialization.

K16, but not K6, Promotes the Formation of Short 10-nm Filaments In Vitro

To investigate whether the properties of K6 and K16 are inherently compatible with the reorganization of keratin filaments characteristic of suprabasal keratinocytes located at the wound edge, we assessed their assembly properties in a purified recombinant form in vitro and when coexpressed in a nonepithelial cell line in culture. The human K6b and K16 coding sequences (see Materials and Methods) were subcloned in vectors for expression in bacteria. Upon transformation of pET-K6b and pET-K16 in the *E. coli* BL21(DE3) strain and induction of recombinant protein expression with IPTG, protein products of size 56 and 48 kD accumulated as inclusion bodies (data not shown). SDS-PAGE/immunoblotting indicated that the recombinant proteins purified by anion-exchange chromatography comigrate with native human K6 and K16 from cultured human epidermal cell extracts (Fig. 3), and react specifically with polyclonal antisera raised against oligopeptides corresponding to the carboxy-terminal portion of K6b (Stoler et al., 1988) and K16 (Takahashi et al., 1994) (Fig. 3). On the basis of properties such as solubility, charge, size, and immunoreactivity, we conclude that the two bacterial strains engineered produce the recombinant forms of human K6b and K16. For the assembly studies described below we used the K5-K14 pair as a reference since: (*a*) they are constitutively expressed in epidermis; (*b*) they are very related to K6 and K16 at the protein sequence level (e.g., Rosenberg et al., 1988; Lersch et al., 1989); and (*c*) their assembly properties are well characterized (Coulombe and Fuchs, 1990). The bacterial strains for the production of recombinant human K5 and K14 have been described before (Coulombe and Fuchs, 1990).

First, mixtures of purified recombinant K5-K14, K6b-

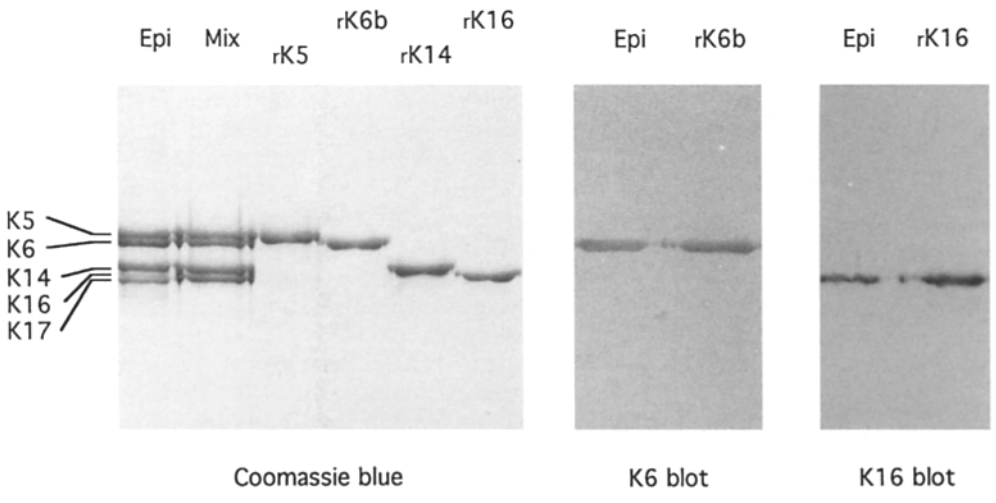

Figure 3. Purification of human recombinant K6b and K16. The human K5, K6b, K14, and K16 cDNAs were expressed in *E. coli* and recombinant proteins were recovered as inclusion bodies, solubilized in Q buffer and purified by anion-exchange chromatography. (*Left*) SDS-PAGE/Coomassie blue staining. The lanes are as follows: Epi, 5 μg of native keratins extracted from cultured human SCC-13 keratinocytes; Mix, mixture containing 1 μg of each of the four purified recombinant keratins; rK5, 1 μg of purified recombinant human K5; rK6b, 1 μg of purified recombinant human K6b; rK14, 1 μg of purified recombinant human K14; rK16, 1 μg of purified recombinant human K16. (*Right*) SDS-PAGE followed by immunoblotting with polyclonal antisera directed against either K6 (K6 blot) or K16 (K16 blot). The lanes are as follows: Epi, 0.15 μg (K6 blot) or 0.5 μg (K16 blot) of native keratins from human SCC-13 keratinocytes; rK6b (50 ng) and rK16 (50 ng) refer to the purified recombinant keratins, as above. The recombinant human K6b and K16 comigrate with their native counterparts, and react with monospecific antisera.

K16, K6b-K14, and K5-K16 were subjected to anion-exchange chromatography in the presence of 6.5 M urea to isolate type I-type II heterotypic complexes (Coulombe and Fuchs, 1990), and chemically cross-link them with BS3 (Geisler et al., 1992). Under these conditions, the K5-K14 and K6b-K14 samples were cross-linked into a single major product of ~240 kD (Fig. 4), indicating efficient heterotetramer formation under these buffer conditions (Coulombe and Fuchs, 1990). In contrast, the K5-K16 and especially the K6b-K16 samples showed significant amounts of a ~135-kD product, corresponding to the heterodimer (Coulombe and Fuchs, 1990), as well as uncross-linked monomers. Identical results were obtained with glutaraldehyde as the cross-linking agent (not shown). No shift in apparent molecular mass occurred when each of the four individually purified keratins was treated with BS3 under identical conditions (not shown). To further test the stability of these heterotypic complexes, we raised the concentration of urea to 8 M. Under these conditions, the yield of the ~240 kD heterotetramer was significantly reduced in the samples featuring K16, while the amount of uncross-linked monomers increased (Fig. 4). These studies showed that K6b/K16 form less stable heterotypic complexes compared to K5/K14, and furthermore that K16 appears to play the major role in this phenomenon. In a parallel set of experiments in which native heterotypic complexes from cultured human epidermal cells were analyzed, K16-containing tetramers were found to be more easily dissociated compared to K14- and K17-containing ones when subjected to anion-exchange chromatography in the presence of urea (data not shown; see Stoler et al., 1988; Rosenberg et al., 1988). This indicate that native human K14 and K16 behave similarly to their respective recombinant counterpart under these conditions.

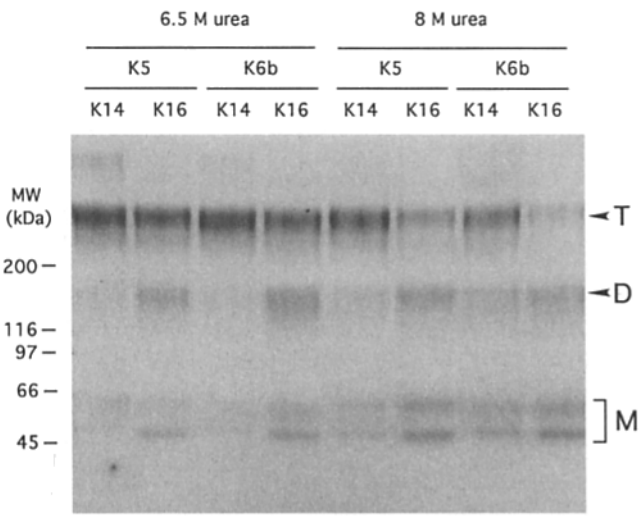

Figure 4. Chemical cross-linking of type I-type II keratin heterotypic complexes. Type I-type II heterotypic complexes were isolated by anion-exchange chromatography and dialyzed against 25 mM sodium phosphate buffer containing either 6.5 or 8 M urea at pH 7.4. Protein concentration was then adjusted to 200 $\mu g \cdot ml^{-1}$, and BS3 was added to a final concentration of 10 mM and the samples incubated for 1 h. at 12°C. Cross-linked products were resolved on a 3–17.5% gradient SDS-PAGE and stained with Coomassie Blue. The migration of molecular mass standards is indicated at left, while that of the type I-type II tetramer (*T*; ~240 kD), type I-type II dimer (*D*; ~135 kD) and type I and type II monomers (*M*) is indicated at right. The K5-K14 combination and to a slightly lesser extent, the K6b-K14 combination form stable heterotetramers that persist even in the presence of 8 M urea. In contrast, substantial amounts of dimers and uncross-linked monomers are found in the K5-K16 and especially the K6b-K16 combinations in the presence of 8 M urea, indicating that these heterotetramers are significantly less stable. Thus, K5-K14 and K6b-K16 formed the most and the least stable heterotetramers, respectively, under these conditions.

Uncross-linked heterotypic complexes were used to examine 10-nm filament assembly. Polymerization was induced by dialysis against assembly buffer, and the products formed were examined by negative staining and electron microscopy. As previously shown (Eichner et al., 1986, Coulombe and Fuchs, 1990), K5-K14 assembled into several micrometer-long filaments having a regular and relatively featureless structure (Fig. 5 *A*). The diameter of K5-K14 filaments was 11.4 ± 1.3 nm (mean ± SD), and they formed with >99% efficiency (as assessed by a filament pelleting assay; see Materials and Methods). The K6b-K14 filaments were indistinguishable from K5-K14 in many respects, including their length (Fig. 5 *B*), diameter (11.3 ± 1.3 nm), and polymerization efficiency (>99%). In contrast, the majority of K6b-K16 filaments were shorter than 1 μm (Fig. 5 *C*) while most K5-K16 filaments were shorter than 0.5 μm (Fig. 5 *D*), although both samples showed considerable length heterogeneity. The K6b-K16 combination assembled with a 90% efficiency, and filaments had a diameter of 11.2 ± 1.2 nm. For the K5-K16 combination, a 88% assembly efficiency and a diameter of 10.6 ± 1.0 nm were measured. Similar results were obtained over a range of protein concentrations (100–400 μg/ml). The K16-containing heterotypic fractions used for filament assembly assays contained a slight molar excess of K16 due to complications in purification arising from the lesser stability of the K16-containing tetramers (e.g., Fig. 4). Since the molar excess of K16 was entirely recovered in the supernatant fraction in the high-speed filament centrifugation assays (see Material and Methods), we presume that it cannot account for the assembly behavior of the K5-K16 and K6b-K16 combinations. Assembly of K5-K14 and K6b-K16 was also tested under buffer conditions known to be optimal for simple epithelial keratins and deletion mutants of K5 and K14 (Wilson et al., 1992), or type III IF proteins. Increasing the ionic strength from 5 to 50 mM Tris-HCl, adding NaCl to 150 mM, or lowering the pH of the buffer did not improve the assembly behavior of K6b-K16 with respect to K5-K14 (not shown). We conclude that under standard in vitro conditions, recombinant K6b and K16 do not show a typical keratin assembly behavior typical of K5-K14 (Coulombe et al., 1990), K1-K10 (Steinert, 1990) and K8-K18 (e.g., Hatzfeld and Weber, 1990). The clearly superior filaments obtained when K6b was copolymerized with K14 indicates that in vitro, K16 is primarily responsible for the formation of shorter 10-nm filaments.

K6 and K16 Form Poorly Extended Filament Arrays in BHK-21 Fibroblasts

We next compared the in vivo assembly properties of K6b-K16, K5-K14, K6b-K14 and K5-K16 in BHK-21 cells. Since

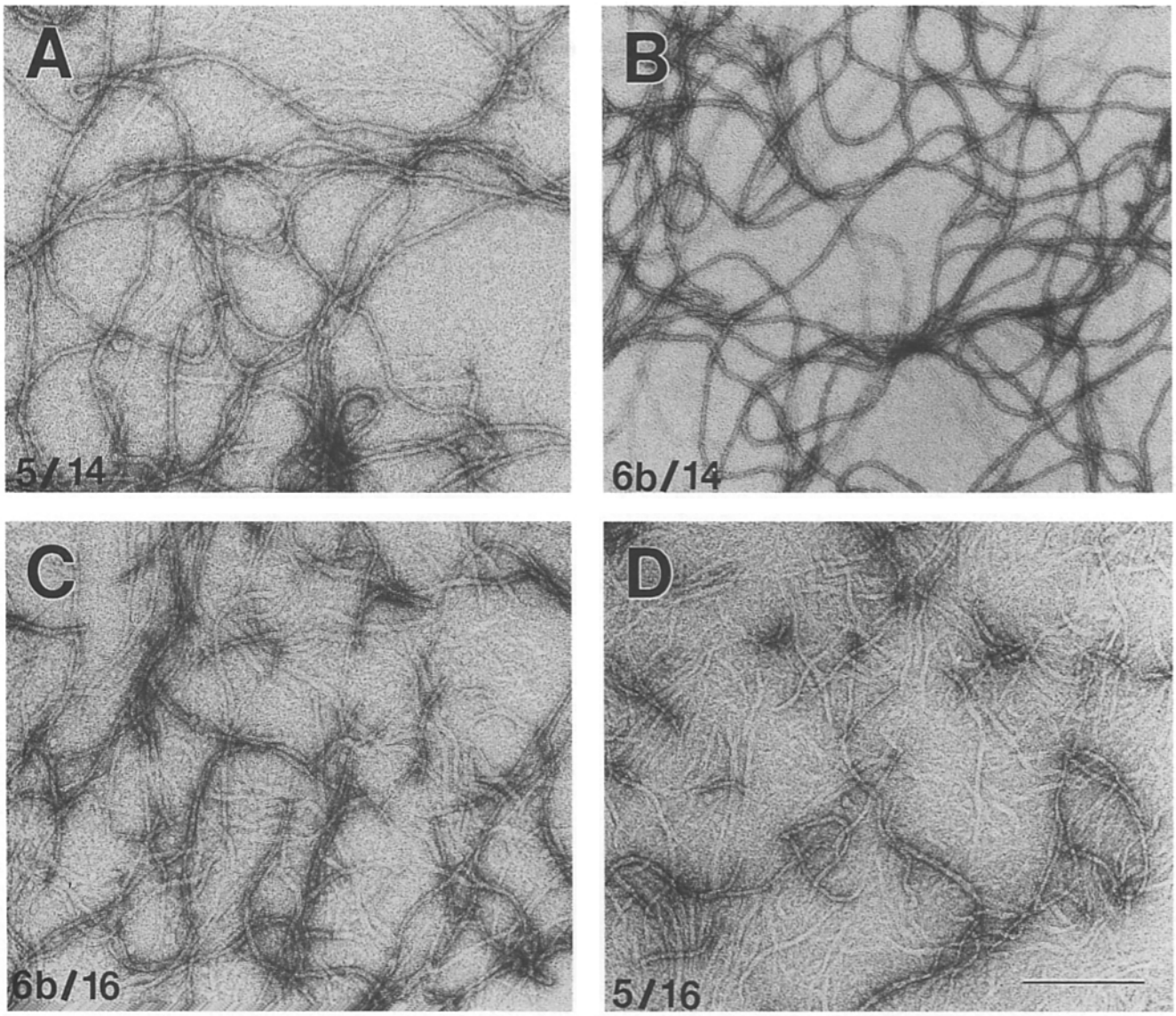

Figure 5. Analysis of reconstituted keratin filaments by electron microscopy. Type I-type II heterotypic complexes were isolated by anion-exchange chromatography and dialyzed against keratin assembly buffer (5 mM Tris-HCl, 10 mM β-ME, pH 7.4) for several hours at 4°C. 5-μl aliquots were applied to glow-discharged carbon-coated grids and negatively stained with uranyl acetate/tylose. Micrographs were recorded on a Zeiss EM10A at a nominal magnification of 31,500×, and magnification was calibrated using a grating replica. *A*, K5-K14; *B*, K6b-K14; *C*, K6b-K16; *D*, K5-K16. While the four type I-type II combinations yielded ~10-nm filaments, their length was clearly dictated by the type I keratin used: K14 led to the assembly of several micron-long IFs, while the filaments containing K16 were typically shorter than 1 μm. See text for details. Bar, 200 nm.

this cell line has a type III (vimentin, desmin) but lacks a keratin IF network (Quinlan and Franke, 1982), it enabled us to examine the ability of human K6b and K16 to polymerize de novo in the cytoplasm of a living cell. Coexpression of K5 and K14 in BHK-21 cells yielded significantly superior cytoplasmic filament arrays compared to NIH 3T3 and CHO cell lines (not shown). When equal amounts of type I (K14 or K16) and type II (K5)-encoding plasmids were mixed in the transfection precipitate, >99% of transfected BHK cells expressed both proteins, as detected by double immunofluorescence staining (not shown). This permitted the use of single-immunofluorescence labelings in experiments involving K6, due to limitations with regards to the species of origin of anti-K6, anti-K14 and anti-K16 antisera (see Materials and Methods).

When K5 and K14 were coexpressed in BHK cells, long bundles of filaments extended throughout the cytoplasm in a majority (>80%) of transfected cells (Fig. 6, *A–C*). These long filament bundles were often oriented along the main axis of the cell (Fig. 6, *A* and *B*). In contrast, a majority of cells (>90%) transfected with K6b and K16 showed loosely packed bundles of filaments that were short and often apposed against the nucleus, forming juxtanuclear aggregates (Fig. 6, *D* and *G*). Fine filaments often radiated from such aggregates, forming thin cytoplasmic processes. The shape of many BHK cells expressing both K6b and K16 appeared to be constricted (Fig. 6 *D*). We did not detect significant differences in the organization of the endogenous vimentin IF network in K5-K14 and K6b-K16–expressing cells, or in nontransfected BHK-21 cells (data

not shown). Preliminary electron microscopy analyses of K6b-K16 transfected cells suggest that the immunopositive juxtanuclear aggregates consist of filaments (data not shown). As seen with K5-K14, coexpression of K6b and K14 led to the formation of an extended array of long filaments in the cytoplasm of transfected cells, showing no preferential association with the surface of the nucleus (Fig. 6, *E* and *H*). Coexpression of K5-K16 in BHK-21 cells resulted in the formation of peculiar arrays consisting of thick and dense bundles of short filaments, often emanating from a juxtanuclear cap (Fig. 6, *F* and *I*). A majority (>80%) of transfected cells displayed such distorted arrays. We repeated these cotransfection experiments using a CMV-K16 gene plasmid construct. No difference in behavior was seen, although the utilization of the cDNA led to higher levels of proteins (as judged from immunostaining intensity; not shown). Of the parameters that could be reliably assessed in these transfection assays, the length and subcellular location of the bundles of filaments forming were clearly determined by the type I keratin involved. As in the in vitro assembly studies, therefore, a clear distinction could be made according to which type I keratin was used in these cotransfection assays. We conclude from these in vivo assembly studies that K6b and K16 do not polymerize into long bundles of filaments that extend throughout the cytoplasm, as seen with the K5-K14 pair. Again, our data suggest that K16 is clearly the primary determinant of this behavior.

Forced Expression of K16 Causes a Retraction of Keratin Filaments in Cultured PtK2 Epithelial Cells

We further compared the assembly properties of human K14 and K16 by expressing them individually in cultured PtK2 cells, which contain a well-extended K8/K18/K19 filament network (Franke et al., 1978). Cells were analyzed by double-immunofluorescence labeling at 24, 48, and 72 h after transfection. In PtK2 cells transfected with the K14 cDNA, the K14 protein integrated into the keratin filament network without disruption (Fig. 7, *A* and *B*). The scoring of several hundred K14-expressing cells at 72 h posttransfection revealed that >85% of them had a completely normal K8-K18 network, consistent with previous studies (e.g., Letai et al., 1992). However, some K14-expressing cells showed an altered organization of K8/K18 filaments. The fact that such cells were rarely seen before the 72 h time point, along with the distinct aggregate-like appearance of the K14-positive material in such cells (an example is shown in Fig. 7 *C*), lead us to conclude that it is due to an excessive expression of an epidermal keratin.

In contrast to K14, expression of the intact K16 cDNA or gene construct in PtK2 cells caused a reorganization of endogenous K8-K18 filaments in a significant fraction of transfected cells (Fig. 7, *E–G*). In many K16-expressing cells, the K8-K18 filament network was retracted from the cytoplasmic periphery, which contained only a few randomly oriented filament bundles. Instead, the bulk of IFs in such cells was found against and around the nucleus. The effects of K16 expression on K8-K18 filament organization appeared to progress in a protein level-dependent fashion, since many more cells were affected at 72 h than at 24 h after transfection, and were clearly different from those seen in the occasional K14-expressing cells showing distinct keratin aggregates (Fig. 7, compare *C* with *D–F*). The scoring of several hundred K16-expressing cells at 72 h posttransfection revealed that >50% of them featured a significantly altered K8-K18 network. We investigated whether the K16-induced retraction of keratin filaments had any effect on the vimentin IF network of PtK2 cells. Double-immunofluorescence labeling indicated no major alteration in the cytoplasmic organization of the vimentin array in K16-expressing cells (data not shown), suggesting that the effects of K16 were specific to the keratin IF network.

Biochemical analyses conducted on PtK2 cells at 72 h following transfection of either CMV-K14 or CMV-K16 established that the correct-size product was synthesized, and furthermore that the average level of epidermal keratin per transfected cell did not differ (Fig. 8). Because the levels of epidermal keratin may vary substantially among transfected cells, this assay does not allow us to quantitate the relative amount of K16 required to induce a retraction of K8/K18 filaments in PtK2 cells. The results obtained in PtK2 cells thus provide additional evidence that the properties of K16 are different than K14. More importantly, they show that expression of K16 at relatively high levels causes a significant reorganization of a preexisting keratin filament network in vivo.

Forced Expression of Human K16 Causes a Reorganization of the Keratin Filament Network in Skin Keratinocytes of Transgenic Mice

We recently reported on a skin phenotype produced when the wild-type human K16 gene (hK16) is overexpressed in transgenic mouse skin (Takahashi et al., 1994). Transgenic animals with low hK16 expression are normal during the first 6 mo of life. In contrast, transgenic mice showing more abundant hK16 expression show aberrant keratinization that begins in the hair follicle outer root sheath and gradually spreads to the proximal epidermis. This phenotype is consistent with the pattern of expression of K16 in human skin (Moll et al., 1982; Stark et al., 1987), and with the fact that the outer root sheath is continuous with the epidermis. In one particular line (5-7), F2 homozygous offsprings (~20 copies of the transgene) develop a severe skin phenotype within a few days after birth. This is unusual among our transgenic animals, since hair follicle morphogenesis and differentiation are not completed until several days after birth (see Kopan and Fuchs, 1989), and can be attributed to an early onset of hK16 expression in the skin of these animals, as documented by histochemistry and western immunoblotting of skin IF extracts (data not shown). The reason for this inappropriate K16 expression in the epidermis of these homozygous pups is not understood, but may involve the saturation of a factor normally responsible for an active repression of K16 gene expression in epidermis (Takahashi et al., 1994).

We examined the epidermis of these 5-7-F2 homozygous K16 transgenic mice at 2 d after birth, before the development of skin lesions, to characterize the morphological consequences of overexpressing K16 in its natural cellular context in vivo, i.e., a skin keratinocyte. Remarkably, at the light microscopy level, dark-staining aggre-

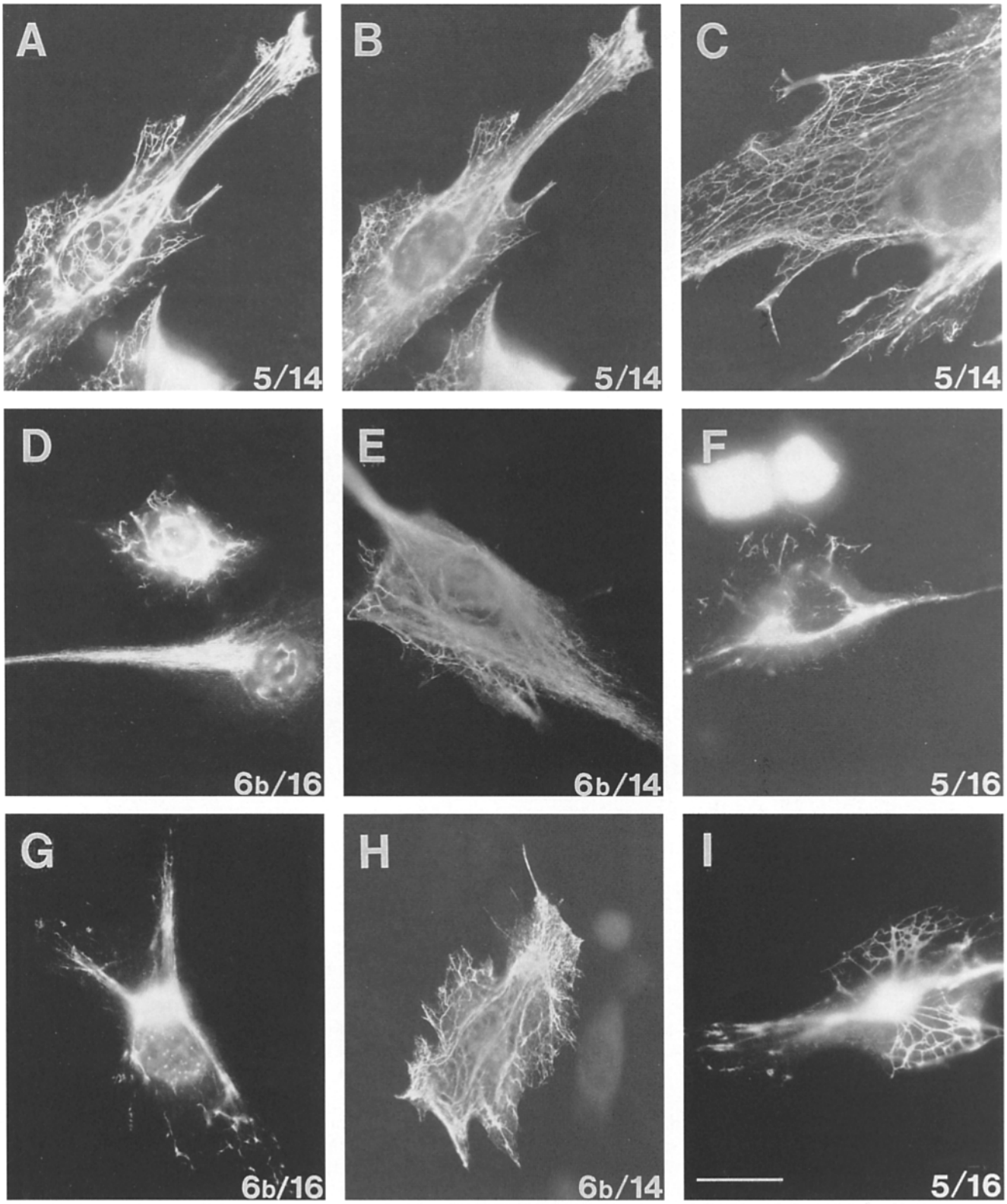

Figure 6. Coexpression of type I and type II keratin cDNAs in fibroblasts. The human K5, K6b, K14, and K16 were subcloned into the GW1-CMV expression vector. Equimolar mixtures of one type I and one type II keratin cDNA-containing plasmids were transfected into BHK-21 cells by the calcium phosphate precipitation method. At 24 h posttransfection, cells were fixed with methanol and processed for single or double-immunofluorescence labelings using primary antisera directed against either K5, K6, K14, or K16, followed by FITC- or Texas Red-conjugated reagents to visualize bound primary antibodies. *A–C*, K5 and K14 coexpressing cells. *A*, anti-K5; *B*, anti-K14 signal of the same cells as in *A*. Note that the two signals colocalize perfectly. *C*, anti-K14 signal in a different transfected cell. *D* and *G*, K6b and K16 coexpressing cells stained with anti-K16. *E* and *H*, K6b and K14 coexpressing cells stained with anti-K14. *F* and *I*, K5 and K16 coexpressing cells stained with anti-K16. In the two type I-type II combinations containing K14, a well-developed array of filament bundles extends throughout the cytoplasm. In contrast, the two combinations containing K16 produce relatively short filament bundles that are apposed against the nucleus. Bar, 25 μm.

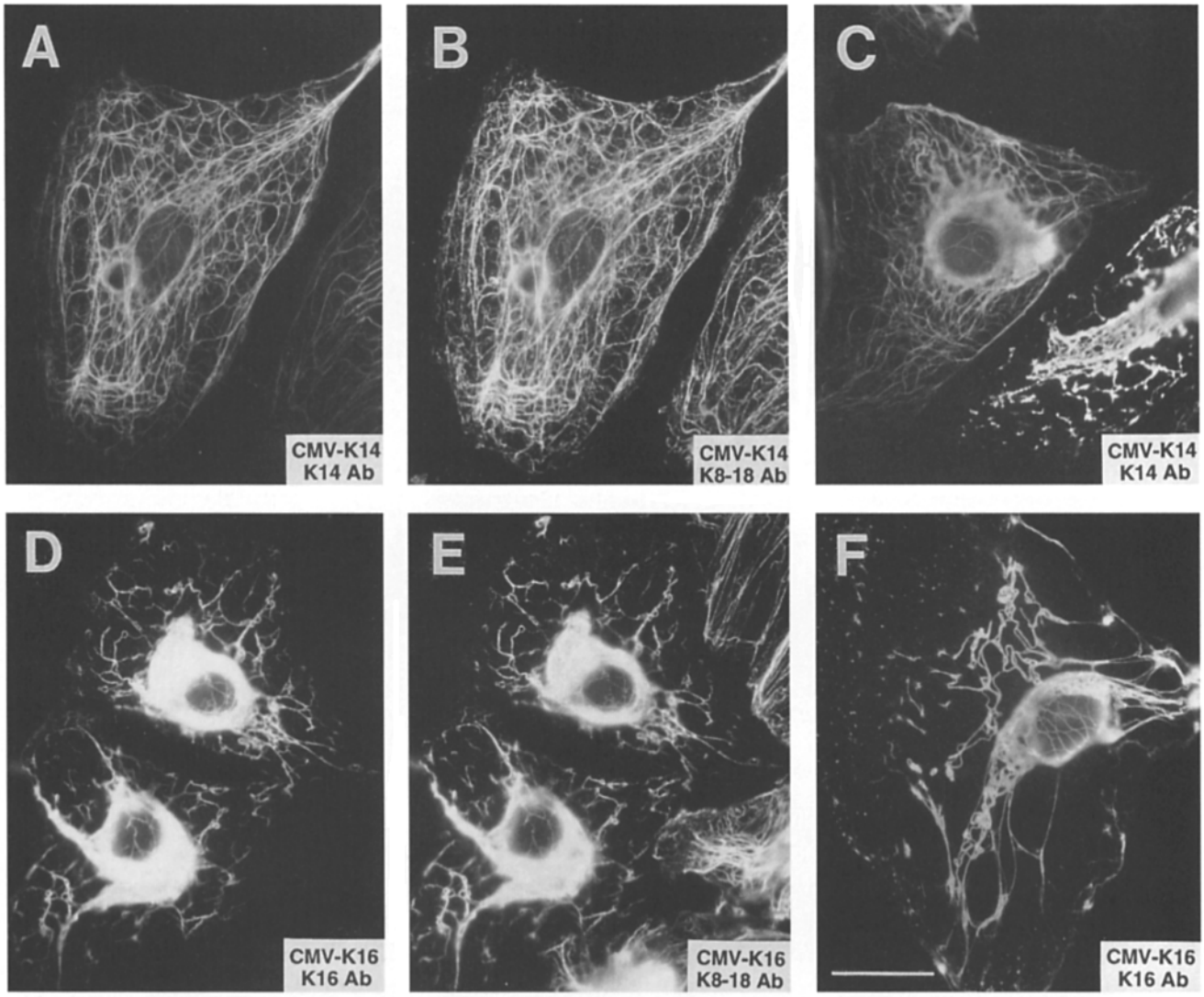

Figure 7. Transient expression of K14 and K16 in cultured PtK2 cells. The human K14 and K16 cDNAs and the human K16 gene were subcloned into the GW1-CMV expression vector and transfected into PtK2 cells by the calcium phosphate precipitation method. At 72 h posttransfection, cells were fixed with methanol and processed for double-immunofluorescence labeling using a monoclonal antibody to K8-K18 and a rabbit antiserum directed against either K14 or K16. Bound primary antibodies were detected by a FITC-conjugated goat anti-rabbit IgG and a goat anti-mouse IgG followed by streptavidin-Texas Red. *A* (anti-K14) and *B* (anti-K8/K18), double-immunofluorescence staining of a cell expressing the K14 cDNA. The K14 protein integrated within the preexisting keratin IF network without perturbing it. While this occurred in the majority of transfected cells, occasional cells showing a very bright staining for K14 featured a disrupted network (*C*, anti-K14). *D* (anti-K16) and *E* (anti-K8/K18), double-immunofluorescence staining of two adjacent cells expressing the K16 cDNA. In these two cells as in >50% of transfected PtK2 cells, the expression of K16 leads to a retraction of keratin filaments from the cell periphery. As shown in *F* (anti-K16 staining), similar results were obtained when a full-length human K16 genomic clone was expressed in PtK2 cells. Bar, 25 μm.

gates of proteins were easily distinguishable around the nucleus of several suprabasal keratinocytes in the epidermis of K16-transgenic but not in control mice (Fig. 9, *A* and *B*). At the electron microscopy level, the dark-staining material in suprabasal keratinocytes of K16 transgenic mice was identified as densely packed keratin filaments (Fig. 9 *C*). Elsewhere in these cells, large areas of cytoplasm show a relative depletion of keratin filaments (Fig. 9 *C*). This ultrastructure contrasts with the homogeneous distribution of keratin filament bundles in non-transgenic keratinocytes (not shown; see Takahashi et al., 1994). The thickness, vertical organization, and ultrastructure of K16 transgenic epidermis is otherwise normal at that stage (compare 9, *A* with *B*), suggesting that the reorganization of keratin filaments is specifically due to K16 overexpression. The formation of juxtanuclear filament aggregates also occurs in the epidermis of other body sites in 5-7-F2 homozygous transgenic animals. These data are important in two respects: first, they indicate that the behavior of K16 in transfected BHK-21 and PtK2 cells is directly relevant to skin keratinocytes in vivo, and second, they strongly support the notion that K16 displays unusual assembly properties, and that its expression at relatively high levels can induce the aggregation of keratin filaments and their

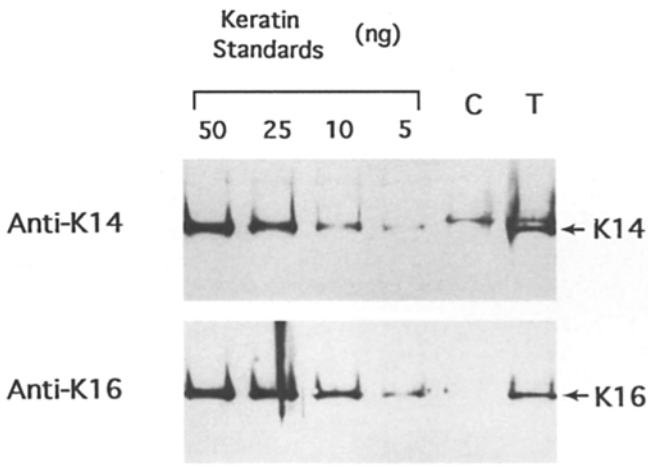

Figure 8. Relative levels of human K14 and K16 protein in transfected PtK2 cells. The CMV-K14 and CMV-K16 cDNAs plasmids, and the GW1-CMV control plasmid, were each transfected into a 100-mm dish of PtK2 cells by the calcium phosphate precipitation method. At 72 h posttransfection, cells were scraped and intermediate filaments were extracted and resolved by SDS-PAGE (1.5 ug total proteins per extract) along with known amounts of FPLC-purified recombinant K14 and K16 (range 5–50 ng). Immunoblotting was performed with anti-K14 (*top*) and anti-K16 (*bottom*) polyclonal antisera diluted at 1:1,000, and bound primary antibodies were detected using enhanced chemiluminescence. Transfection efficiency was measured by immunofluorescence staining of cells cultured on glass coverslips, and found to be similar in K14- and K16-transfected cells (~13–14% in both cases). Likewise, similar amounts of transfected protein occur in K14- and in K16-transfected PtK2 cells (*T* lane). Neither K14 or K16 is detected in the IF extract prepared from CMV plasmid-transfected cells (*C* lane), although the K14 antiserum cross-react with a ~52 kD antigen present in the CMV extract. This analysis indicates that the average levels of K14 and K16 protein per transfected PtK2 cell are similar at the 72 h time point.

reorganization near the nucleus, in a fashion analogous to what is seen in suprabasal keratinocytes of human epidermis subjected to injury (see Fig. 1).

Discussion

The Properties of K16 Suggest a Distinct Function in Skin

Our studies demonstrate that the properties of K16 differ significantly from those of the highly-related K14 with respect to tetramer stability and 10-nm filament structure and organization. Expression of K16 in BHK-21 cells, a non-epithelial cell host, in PtK2 cells, a simple epithelial cell host, and in transgenic mouse keratinocytes results in the aggregation of keratin filaments near the surface of the nucleus in a significant fraction of cells. Reorganization of keratin filaments occurred whether the K16 cDNA or genomic clone was used, and whether K5, K6b, or K8 was involved as the type II assembly partner. In contrast, K6b showed standard assembly properties when copolymerized with K14 in vitro and in cultured fibroblasts. Among the known human K6 isoforms (Takahashi et al., 1995), it is K6a that predominates at the mRNA level in normal skin tissue, in squamous cell carcinoma of the skin, and in cultured skin explants (Tyner et al., 1986; Takahashi et al., 1995). It is therefore conceivable that K6a is a more suitable assembly partner for K16, although K6a and K6b are predicted to differ at only seven amino acid positions (Takahashi et al., 1995). Further experimentation is needed to test this possibility. Our findings strongly suggest that K6b and K16 are fundamentally different from other known keratin pairs, such as K8-K18 (Hatzfeld and Weber, 1990; Lu and Lane, 1990; Bader et al., 1991), K5-K14 (Coulombe and Fuchs, 1990; this study), and even K1-K10 (Steinert, 1990; Blessing et al., 1993), although there is evidence that these latter do not form an extended IF array when expressed in nonkeratinocytes in culture (Kartasova et al., 1993; Paramio et al., 1994). Our data also suggest that K16 is primarily responsible for the assembly behavior of the K6b-K16 combination. These results imply that the intrinsic assembly properties of K16 may not be optimal for a function of mechanical support akin to the main epidermal keratins. Consistent with this notion, the skin lesions caused by human K16 overexpression in transgenic mice (Takahashi et al., 1994), or associated with point mutations in the human K16 sequence in pachyonychia congenita and focal keratoderma diseases (Shamsher et al., 1995; McLean et al., 1995) are not associated with cytolysis, unlike the blistering disorders caused by similar mutations in keratin genes that are constitutively expressed in epidermis (e.g., Fuchs et al., 1994). In addition, the polarized reorganization of keratin filaments that occurs at the epidermal wound edge, and which correlates with the accumulation of K6, K16, and K17, is distinct from the disruption of keratin filaments typical of skin blistering disorders. Studies involving transgenic mouse models will be necessary to directly test the notion that K16 and epidermal type I keratins such as K14 and K10 can not functionally substitute for one another in skin keratinocytes, normal and when challenged by injury. The actual demonstration of a distinct function for K16 during wound healing would have important implications for the functional significance of keratin and intermediate filament sequence diversity (for a recent discussion see Klymkowsky, 1995).

Changes in Keratin Expression May Be Necessary before Onset of Re-Epithelialization: Defining a Potential Role for Keratin 16

As they undergo differentiation, epidermal keratinocytes mature into the highly specialized squame, a key contributor to both the properties and function of skin. The main structural element of the fully differentiated keratinocyte is keratin (~85% of its total protein), and a major fraction of it consists of K1 and K10 (Fuchs and Green, 1980; Moll et al., 1982). K1 and K10 are high molecular mass keratins (67 and 56.6 kD, respectively; Moll et al., 1982) whose pairwise expression is specific to cornifying epithelia. In epidermis in situ, expression of K1 and K10 occurs early after engagement into differentiation (i.e., they are easily detected in the first layer of suprabasal epidermal cells), and correlates with a marked propensity of 10-nm keratin filaments to laterally associate and form dense bundles (Coulombe et al., 1989). Formation of these filament bundles clearly precedes the synthesis of filaggrin, a known fil-

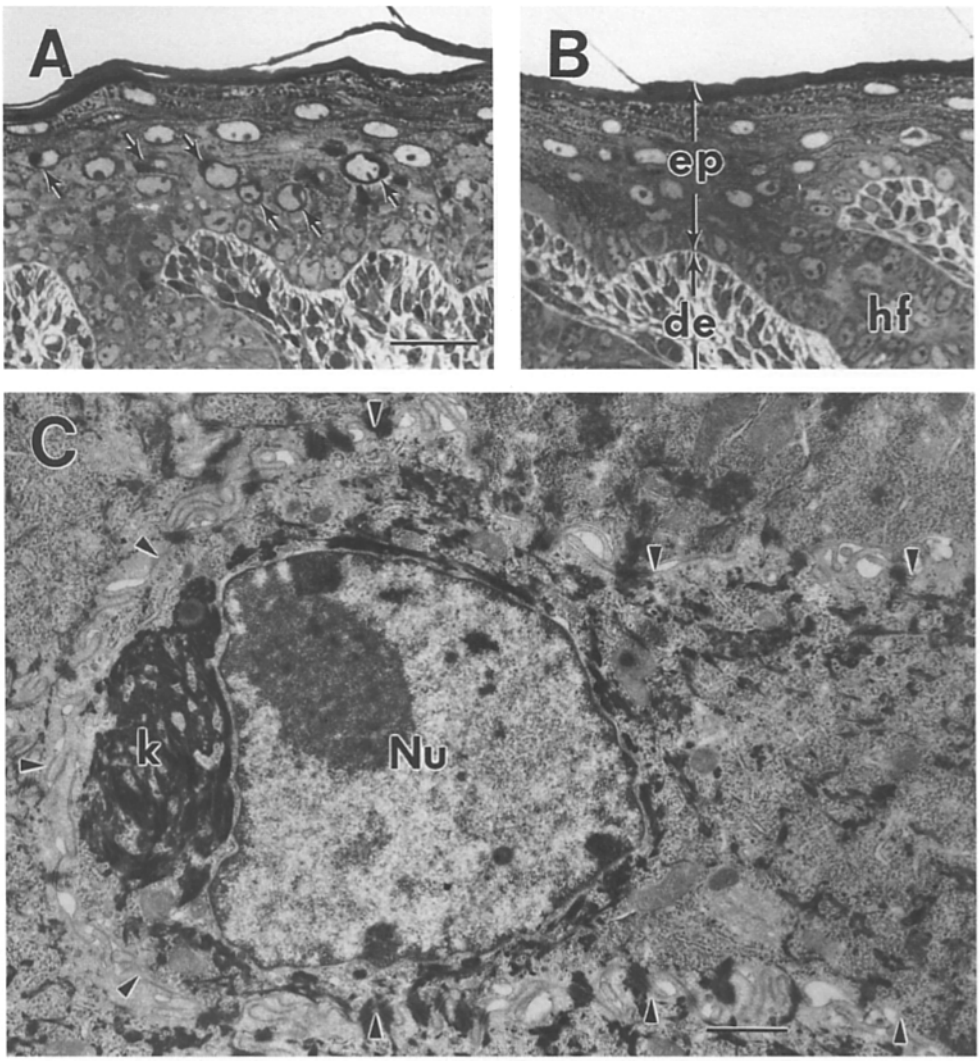

Figure 9. Overexpression of human K16 causes a juxtanuclear reorganization of keratin filaments in suprabasal keratinocytes of transgenic mouse skin. (*A* and *B*) Light microscopy of toluidine-blue stained sections prepared from epoxy-embedded skin samples of 2 d-old mouse pups. (*A*) 5-7-F2 homozygous K16 transgenic pup, whose epidermis express the human K16 transgene suprabasally (not shown). (*B*) Control (non-transgenic) pup from the same litter. The thickness and architecture of the two epidermises are normal. Note, however, the occurrence of dark-staining material around the nucleus of many suprabasal keratinocytes in transgenic epidermis (*A*, *arrows*). This material is completely absent in control epidermis (*B*). (*C*) Electron microscopy of the transgenic epidermis shown in *A*. The arrowheads depict the outline of a suprabasal keratinocyte in which a large mass of aggregated keratin filaments (*k*) lies against the nucleus (*Nu*). The remainder of the cytoplasm contains unusually low amounts of keratin filament bundles. Consistent with the histology shown in frame A, many additional suprabasal cells show aggregated keratin filaments near the nucleus. Bars: (*A* and *B*) 25 μm; (*C*) 1 μm.

ament aggregating activity expressed in late differentiating keratinocytes (Dale et al., 1985). Interestingly, K1 and K10 show a natural tendency to form filament aggregates or bundles when copolymerized in vitro (Eichner et al., 1986), when coexpressed in pancreatic β-cells of transgenic mice (Blessing et al., 1993) and in other cell types in culture (Kartasova et al., 1993; Paramio et al., 1994), suggesting that they have the intrinsic ability to promote such filament bundling. Given that keratin filaments are anchored at the surface of the nucleus and at desmosomes at the cell periphery, it is conceivable that the filament bundling so adeptly promoted by K1 and K10 may contribute to the flattening of keratinocytes that occurs as they differentiate. At later stages of differentiation, the covalent cross-linking of keratin to the cornified cell envelope (Steinert and Marekov, 1995) is likely to further promote the progression of keratinocytes towards the omelet-shaped cell characteristic of granular cells. It follows that the properties of K1 and K10 are attuned to the needs and fate of a differentiating epidermal cell (see Blessing et al., 1993, for discussion).

Epidermal keratinocytes involved in re-epithelialization share few of the defining features of a terminally differentiating cell, notably cell shape, cell–cell adhesion, and cytoarchitecture, including the organization of keratin filaments (this study; also, see Odland and Ross, 1968; Gabbiani et al., 1978). It is widely believed that keratinocytes from both the basal and spinous layers of epidermis and outer root sheath of hair follicles (in the case of partial skin thickness wounds) participate to re-epithelialization of injured mammalian skin (see Stenn and DePalma, 1988; Clark, 1993). Garlick and Taichman (1994) recently showed that genetically marked suprabasal keratinocytes at the wound edge are recruited for the re-epithelialization of wounded keratinocyte raft cultures. The model of re-epithelialization currently in favor states that within the migrating epithelial sheet, keratinocytes "roll" over one another in a leapfrog fashion so that leading cells are successively implanted as new basal cells (Krawczyk, 1971; Winter, 1972; see Bereiter-Hahn, 1984; Clark, 1993). This rolling mechanism has several implications (see below), an important one being that spinous keratinocytes must be re-programmed to become competent for re-epithelialization (keratinocyte activation; see Grinnell, 1992), a situation where they are in an unusually dynamic state. Based on their properties, it is unlikely that maintenance of K1/

K10-rich keratin filament network would be compatible with normal re-epithelialization. Accordingly, spinous keratinocytes at the epidermal wound edge display reduced levels of K10 protein (this study; Mansbridge and Knapp, 1987; Coulombe et al., 1991). From our results, we propose that the induction of K16 (and possibly K6, K17) is involved in enabling the differentiating keratinocyte to become competent for re-epithelialization. This concept is rooted in the observations that: (*a*) accumulation of K6 and K16 (and K17 later on) correlates with the acquisition of an activated phenotype in suprabasal keratinocytes located at the wound edge; (*b*) K16 does not show conventional keratin assembly behavior under in vitro and ex vivo conditions; and (*c*) overexpression of K16 in the skin of transgenic mice can cause many of the cytoarchitectural changes typical of the wound edge at 18–30 h after injury. Accumulation of K16 could play a role in the initial aggregation of existing keratin filament bundles in spinous keratinocytes located at the wound edge, which occurs between 12 and 18 h after injury. Subsequently, these spinous keratinocytes adopt an elongated shape and develop a distinct polarity with respect to the wound site, in preparation for cell migration. Studies involving gene inactivation in mouse will be required to test the hypothesis that K16 (and possibly K6, K17) plays a vital permissive role during wound healing, and in particular, that the accumulation of K16 contributes to the reorganization of keratin filaments in wound edge keratinocytes.

While the properties of K16 we uncovered appear compatible with a function of modulation of keratin filament organization, there is available evidence that does not directly support this notion. For instance, K16 in constitutively expressed in a number of stratified epithelia, including hair follicle outer root sheath, palmar and plantar epidermis, tongue and oral mucosa (Moll et al., 1982; 1983; O'Guin et al., 1990), without apparent consequences for the organization of keratin filaments. While additional studies will be necessary to resolve this apparent paradox, there are a number of potential solutions which can be offered at the present time. A key element that could control the effects of K16 expression may reside in the stoichiometry between the type I keratins present in a given epithelial cell. According to this scheme, a cytoplasmic "concentration threshold" would have to be exceeded before the properties of K16 are manifested in a detectable fashion. At the proximal edge of wounded epidermis, for instance, the levels of K16 protein would be unusually high relative to other type I keratins such as K10 (as suggested but not proven by our data), and accordingly the reorganization of keratin filaments would be most obvious. Conversely, in epithelial cells known to express K16 constitutively, its levels relative to other type I keratins would be comparatively low, such that its effect on filament organization would be difficult to ascertain. This "stoichiometry argument" is at least partly supported by biochemical data from normal epithelial tissues such as hair follicle outer root sheath, sweat gland ducts, and plantar epidermis (e.g., Moll et al., 1983; Knapp et al., 1986; Yoshikawa et al., 1995). Together with the relatively lower stability of type I-type II heterotypic complexes involving K16 (our study), such low levels of K16 protein would safeguard the normal keratinocyte against the undesirable consequences of its expression in normal epithelia. An alternative to the stoichiometry argument is the possible existence of an additional human K16 gene (as discussed by McLean et al., 1995, and Paladini et al., 1995), distinct from the one used in our study, which would encode a K16 isoform with properties better suited for normal epithelial cells. Yet another explanation resides in the potential existence of factors such as posttranslational modifications and associated proteins that could differentially modulate the properties of K16 under various biological contexts. As mentioned above, additional studies will be required to examine these and other possibilities.

Implications for the Cellular Mechanisms of Re-Epithelialization

The rolling mechanism of keratinocyte sheet migration (Krawczyk, 1971; Winter, 1972) represents an intriguing hypothesis, primarily because it implies that commitment to differentiation of a basal epidermal cell is not an irreversible process, and possibly, that after their implantation as new basal cells, keratinocytes originating from a post-mitotic stage may resume mitosis again. So far, the evidence in support of the rolling mechanism is indirect and mainly morphological. Thus, suprabasal keratinocytes located at the wound edge (even behind the tongue of migrating epithelium) show an obvious polarity in their cytoarchitecture that suggest their active migration towards the wound site (Alexander, 1981; this study). In addition, the notion that post-mitotically expressed keratins such as K10 (Ortonne et al., 1981; this study), K16 and K17 (this study) are detected in the basal layer of the re-epithelialized wound site is also consistent with this model, although one must consider the alternative that the re-distribution of such biochemical markers is a consequence of altered gene expression instead of a genuine reflection of the origin of the migrating cells. While it appears clear that a subpopulation of suprabasal, post-mitotic keratinocytes is directly involved in the re-epithelialization of epidermis following injury (see above) and undergo significant phenotypic changes while doing so, the extent and the nature of their contribution remains to be ascertained.

The authors are very grateful to Dr. E. Fuchs (University of Chicago) for her generous gift of the human K16 gene and several anti-keratin antibodies, and to M. Delannoy (Johns Hopkins University) for his expertise in thin-sectioning for electron microscopy. We also thank Dr. B. Omary (Stanford University), Dr. B. Dale (University of Washington) for providing antibodies, and Dr. Omary, Dr. K. McGowan (our laboratory), Dr. M. Lee, Dr. J. Porter, and Mr. E. De La Cruz (Johns Hopkins University) for advice and comments.

These studies were supported by grant CB-73 and a Junior Faculty Award (both to P. A. Coulombe) from the American Cancer Society.

Received for publication 12 September 1995 and in revised form 23 October 1995.

References

Alexander, S. A. 1981. Patterns of epidermal cell polarity in healing open wounds. *Ann. Surg. Res.* 31:456–462.

Bader, B. L., T. M. Magin, M. Freudenmann, S. Stumpp, and W. W. Franke. 1991. Intermediate filaments formed de novo from tail-less cytokeratins in the cytoplasm and in the nucleus. *J. Cell Biol.* 115:1293–1307.

Bereiter-Hahn, J. 1984. Epidermal cell migration and wound repair. Biology of the Integument, Vol. 2: Vertebrates. Berlin, Springer-Verlag. 443–471.

Blessing, M., U. Ruther, and W. W. Franke. 1993. Ectopic synthesis of epider-

mal cytokeratins in pancreatic islet cells of transgenic mice interferes with cytoskeletal order and insulin production. *J. Cell Biol.* 120:743–755.

Bradford, M. M. 1976. A rapid and sensitive method for the quantitation of microgram quantities of protein utilizing the principle of protein-dye binding. *Anal. Biochem.* 72:248–254.

Chan, Y.-M., I. Anton-Lampbrecht, Q. C. Yu, A. Jackel, B. Zabel, J. P. Ernst, and E. Fuchs. 1994. A human keratin 14 "knockout": the absence of K14 leads to severe epidermolysis bullosa simplex and a function for an intermediate filament protein. *Genes Dev.* 8:2574–2587.

Chou, C. F., C. L. Riopel, L. S. Rott, and M. B. Omary. 1993. A significant soluble keratin fraction in 'simple' epithelial cells. Lack of an apparent phosphorylation and glycosylation role in keratin solubility. *J. Cell Sci.* 105:433–445.

Clark, R. A. F. 1993. Mechanisms of cutaneous wound repair. *In* Dermatology in General Medicine. T. B. Fitzpatrick, A. Z. Eisen, K. Wolff, I. M. Freedberg, and M. D. Austen, editors. McGraw-Hill, NY. 473–486.

Coulombe, P. A. 1993. The cellular and molecular biology of keratins: beginning a new era. Review. *Curr. Opin. Cell Biol.* 5:17–29.

Coulombe, P. A., and E. Fuchs. 1990. Elucidating the early stages of keratin filament assembly. *J. Cell Biol.* 111:153–169.

Coulombe, P. A., M. E. Hutton, R. Vassar, and E. Fuchs. 1991. A function for keratins and a common thread among different types of epidermolysis bullosa simplex diseases. *J. Cell Biol.* 115:1661–1674.

Coulombe, P. A., R. Kopan, and E. Fuchs. 1989. Expression of keratin K14 in the epidermis and hair follicle: insights into complex programs of differentiation. *J. Cell Biol.* 109:2295–2312.

Croft, C. B., and D. Tarin. 1970. Ultrastructural studies of wound healing in mouse skin. I. Epithelial behavior. *J. Anat.* 106:63–77.

Dale, B. A., K. A. Holbrook, J. R. Kimball, M. Hoff, and T. T. Sun. 1985. Expression of epidermal keratins and filaggrin during human fetal skin development. *J. Cell Biol.* 101:1257–1269.

de Mare, S., P. van Erp, F. C. Ramaekers, and P. vandeKerkhof. 1990. Flow cytometric quantification of human epidermal cells expressing keratin 16 in vivo after standardized trauma. *Arch. Dermatol. Res.* 282:126–130.

Eichner, R., T. T. Sun, and U. Aebi. 1986. The role of keratin subfamilies and keratin pairs in the formation of human epidermal intermediate filaments. *J. Cell Biol.* 102:1767–1777.

Franke, W. W., E. Schmid, M. Osborn, and K. Weber. 1978. Different intermediate-sized filaments distinguished by immunofluorescence microscopy. *Proc. Natl. Acad. Sci. USA.* 75:5034–5038.

Fuchs, E. 1993. Epidermal differentiation and keratin gene expression. *J. Cell Sci.* (Suppl). 17:197–208.

Fuchs, E., and P. A. Coulombe. 1992. Of mice and men: Genetic skin diseases of keratin. *Cell.* 69:899–902.

Fuchs, E., P. A. Coulombe, J. Cheng, Y.-M. Chan, E. Hutton, A. Syder, L. Degenstein, Q. C. Yu, A. Letai, and R. Vassar. 1994. Genetic bases of epidermolysis bullosa simplex and epidermolytic hyperkeratosis. *J. Invest. Dermatol.* 103:25S–30S.

Fuchs, E., and H. Green. 1980. Changes in keratin gene expression during terminal differentiation of the keratinocyte. *Cell.* 19:1033–1042.

Fuchs, E., and K. Weber. 1994. Intermediate filaments: structure, dynamics, function, and disease. *Ann. Rev. Biochem.* 63:345–382.

Gabbiani, G., C. Chaponnier, and I. Hüttner. 1978. Cytoplasmic filaments and gap junctions in epithelial cells and myofibroblasts during wound healing. *J. Cell Biol.* 76:561–568.

Garlick, J. A., and L. B. Taichman. 1994. Fate of human keratinocytes during re-epithelialization in an organotypic culture model. *Lab. Invest.* 70:916–924.

Geisler, N., J. Schunemann, and K. Weber. 1992. Chemical cross-linking indicates a staggered and antiparallel protofilament of desmin intermediate filaments and characterizes one higher-level complex between protofilaments. *Eur. J. Biochem.* 206:841–852.

Grinnell, F. 1992. Wound repair, keratinocyte activation, and integrin modulation. *J. Cell Sci.* 101:1–5.

Hatzfeld, M., and K. Weber. 1990. The coiled coil of in vitro assembled keratin filaments is a heterodimer of type I and II keratins: use of site-specific mutagenesis and recombinant protein expression. *J. Cell Biol.* 110:1199–1210.

Hotchin, N. A., N. L. Kovach, and F. M. Watt. 1993. Functional down-regulation of alpha 5 beta 1 integrin in keratinocytes is reversible but commitment to terminal differentiation is not. *J. Cell Sci.* 106:1131–1138.

Kartasova, T., D. R. Roop, K. A. Holbrook, and S. H. Yuspa. 1993. Mouse differentiation-specific keratins 1 and 10 require a preexisting keratin scaffold to form a filament network. *J. Cell Biol.* 120:1251–1261.

Klymkowsky, M. W. 1995. Intermediate filaments: new proteins, some answers, more questions. *Curr. Opin. Cell Biol.* 7:46–54.

Knapp, A. C., W. W. Franke, H. Heid, M. M. Hatzfeld, J. L. Jorcano, and R. Moll. 1986. Cytokeratin No. 9, an epidermal type I keratins characteristic of a special program of keratinocyte differentiation displaying body-site specificity. *J. Cell Biol.* 103:657–667.

Kopan, R., and E. Fuchs. 1989. A new look into an old problem: keratins as tools to investigate determination, morphogenesis, and differentiation in skin. *Genes & Dev.* 3:1–15.

Krawczyk, W. S. 1971. A pattern of epidermal cell migration during wound healing. *J. Cell Biol.* 49:247–263.

Lersch, R., V. Stellmach, C. Stocks, G. Giudice, and E. Fuchs. 1989. Isolation, sequence, and expression of a human keratin K5 gene: transcriptional regulation of keratins and insights into pairwise control. *Mol. Cell. Biol.* 9:3685–3697.

Letai, A., P. A. Coulombe, and E. Fuchs. 1992. Do the ends justify the mean? Proline mutations at the ends of the keratin coiled-coil rod segment are more disruptive than internal mutations. *J. Cell Biol.* 116:1181–1195.

Lloyd, C., Q. C. Yu, J. A. Cheng, K. Turksen, L. Degenstein, L. Hutton, and E. Fuchs. 1995. The basal keratin network of stratified squamous epithelia: defining K15 function in the absence of K14. *J. Cell Biol.* 129:1329–1344.

Lowthert, L. A., N. O. Ku, J. Liao, P. A. Coulombe, and B. Omary. 1995. Empigen BB: A useful detergent for solubilization and biochemical analysis of keratins. *Biochem. Biophys. Res. Commun.* 206:370–379.

Lu, X., and E. B. Lane. 1990. Retrovirus-mediated transgenic keratin expression in cultured fibroblasts: specific domain functions in keratin stabilization and filament formation. *Cell.* 62:681–696.

Mansbridge, J. N., and A. M. Knapp. 1987. Changes in keratinocyte maturation during wound healing. *J. Invest. Dermatol.* 89:253–263.

Matoltsy, A. G. 1955. In vitro wound repair of adult human skin. *Anat. Res.* 122: 581–587.

McLean, W., and E. B. Lane. 1995. Intermediate filaments in diseases. *Curr. Opin. Cell Biol.* 7:118–125.

McLean, W. H. I., E. L. Rugg, D. P. Lunny, S. M. Morley, E. B. Lane, O. Swensson, P. J. C. Dopping-Hepenstal, W. A. D. Griffiths, R. A. J. Eady, C. Higgins, et al. 1995. Keratin 16 and keratin 17 mutations cause pachyonychia congenita. *Nature Genetics.* 9:273–278.

Moll, R., W. W. Franke, D. L. Schiller, B. Geiger, and R. Krepler. 1982. The catalog of human cytokeratins: patterns of expression in normal epithelia, tumors and cultured cells. *Cell.* 31:11–24.

Moll, R., R. Krepler, and W. W. Franke. 1983. Complex cytokeratin polypeptide patterns observed in certain human carcinomas. *Differentiation.* 23:256–269.

Nelson, W. G., and T. T. Sun. 1983. The 50- and 58-kilodalton keratin classes as molecular markers for stratified squamous epithelia: cell culture studies. *J. Cell Biol.* 97:244–251.

Odland, G., and R. Ross. 1968. Human wound repair. I. Epidermal regeneration. *J. Cell Biol.* 39:135–151.

O'Guin, W. M., A. Schermer, M. Lynch, and T.-T. Sun. 1990. Differentiat ion-specific expression of keratin pairs. *In* Cellular and Molecular Biology of Intermediate Filaments. R. D. Goldman and P. M. Steinert, editors. Plenum Publishing Corp. 301–334.

Ortonne, J. P., T. Loning, D. Schmitt, and J. Thivolet. 1981. Immunomorphological and ultrastructural aspects of keratinocyte migration in epidermal wound healing. *Virch. Arch. Path. Anat.* 392:217–230.

Paladini, R. D., K. Takahashi, T. M. Gant, and P. A. Coulombe. 1995. cDNA cloning and bacterial expression of the human type I keratin 16. *Biochem. Biophys. Res. Commun.* 215:517–523.

Paramio, J. M., and J. L. Jorcano. 1994. Assembly dynamics of epidermal keratins K1 and K10 in transfected cells. *Exp. Cell Res.* 215:319–331.

Quinlan, R. A., and W. W. Franke. 1982. Heteropolymer filaments of vimentin and desmin in vascular smooth muscle tissue and cultured baby hamster kidney cells demonstrated by chemical crosslinking. *Proc. Natl. Acad. Sci. USA.* 79:3452–3456.

Rice, R. H., and H. Green. 1979. Presence in human epidermal cells of a soluble protein precursor of the cross-linked envelope: activation of the cross-linking by calcium ions. *Cell.* 18:681–694.

Rosenberg, M., A. RayChaudhury, T. B. Shows, B. M. Le, and E. Fuchs. 1988. A group of type I keratin genes on human chromosome 17: characterization and expression. *Mol. Cell. Biol.* 8:722–736.

Rugg, E. L., I. W. H. McLean, E. B. Lane, R. Pitera, J. R. McMillan, P. J. C. Dopping-Hepenstal, H. A. Navsaria, I. M. Leigh, and R. A. J. Eady. 1994. A functional "knockout" of human keratin 14. *Genes & Dev.* 8:2563–2573.

Schermer, A., J. V. Jester, C. Hardy, D. Milano, and T. T. Sun. 1989. Transient synthesis of K6 and K16 keratins in regenerating rabbit corneal epithelium: keratin markers for an alternative pathway of keratinocyte differentiation. *Differentiation.* 42:103–110.

Shamsher, M. K., H. A. Navsaria, H. P. Stevens, R. C. Ratnavel, P. E. Purkis, D. P. Kelsell, W. H. I. McLean, L. J. Cook, W. A. D. Griffiths, N. Spurr, and I. M. Leigh. 1995. Novel mutations in keratin 16 gene underlie focal non-epidenmolytic palmoplantar keratoderma (NEPPK) in two families. *Hum. Molec. Genet.* 4:1875–1881.

Stark, H. J., D. Breikreutz, A. Limat, P. Bowden, and N. E. Fusenig. 1987. Keratins of the human hair follicle: "hyperproliferative" keratins consistently expressed in outer rrot sheath cells in vivo and in vitro. *Differentiation.* 35: 236–248.

Steinert, P. M. 1990. The two-chain coiled-coil molecule of native epidermal keratin intermediate filaments is a type I-type II heterodimer. *J. Biol. Chem.* 265:8766–8774.

Steinert, P. M., and L. N. Marekov. 1995. The proteins elafin, filaggrin, keratin intermediate filaments, loricrin and small proline-rich proteins 1 and 2 are isodipeptide cross-linked components of the human epidermal cornified envelope. *J. Biol. Chem.* 270:17702–17711.

Stenn, K. S., and L. DePalma. 1988. Re-epithelialization. *In* The Molecular and Cellular Biology of Wound Repair. R. A. F. Clark, and P. M. Henson, editors. Plenum Press, NY. 321–335.

Stoler, A., R. Kopan, M. Duvic, and E. Fuchs. 1988. Use of monospecific antisera and cRNA probes to localize the major changes in keratin expression during normal and abnormal epidermal differentiation. *J. Cell Biol.* 107:427–446.

Studier, F. W., A. H. Rosenberg, J. J. Dunn, and J. W. Dubendorff. 1990. Use of T7 RNA polymerase to direct expression of cloned genes. *Methods Enzy-*

mol. 185:60–89.

Takahashi, K., J. Folmer, and P. A. Coulombe. 1994. Increased expression of keratin 16 causes anomalies in cytoarchitecture and keratinization in transgenic mouse skin. *J. Cell Biol.* 127:505–520.

Takahashi, K., R. Paladini, and P. A. Coulombe. 1995. Cloning and characterization of multiple human genes and cDNAs encoding highly related type II keratin 6 isoforms. *J. Biol. Chem.* 270:18581–18592.

Tyner, A. L., M. J. Eichman, and E. Fuchs. 1985. The sequence of a type II keratin gene expressed in human skin: conservation of structure among all intermediate filament genes. *Proc. Natl. Acad. Sci. USA.* 82:4683–4687.

Tyner, A. L., and E. Fuchs. 1986. Evidence for posttranscriptional regulation of the keratins expressed during hyperproliferation and malignant transformation in human epidermis. *J. Cell Biol.* 103:1945–1955.

Viziam, C. B., A. G. Matoltsy, and H. Mescon. 1964. Epithelialization of small wounds. *J. Invest. Dermatol.* 43:499–507.

Weiss, R. A., R. Eichner, and T. T. Sun. 1984. Monoclonal antibody analysis of keratin expression in epidermal diseases: a 48- and 56-kilodalton keratin as molecular markers for hyperproliferative keratinocytes. *J. Cell Biol.* 98:1397–1406.

Wilson, A. K., P. A. Coulombe, and E. Fuchs. 1992. The roles of K5 and K14 head, tail, and R/K L L E G E domains in keratin filament assembly in vitro. *J. Cell Biol.* 119:401–414.

Winstanley, E. W. 1975. The epithelial reaction in the healing of excised cutaneous wounds in the dog. *J. Compar. Pathol.* 85:61–75.

Winter, G. D. 1962. Formation of the scab and the rate of epithelialization of superficial wounds in the skin of the young domestic pig. *Nature (Lond.).* 193:293–294.

Winter, G. D. 1972. Epidermal regeneration studied in the domestic pig. *In* Epidermal Wound Healing. H.I. Maibach, and D.T. Rovee, editors. Year Book Medical Publishing, Chicago. 71–113.

Wu, Y. J., L. M. Parker, N. E. Binder, M. A. Beckett, J. H. Sinard, C. T. Griffiths, and J. G. Rheinwald. 1982. The mesothelial keratins: a new family of cytoskeletal proteins identified in cultured mesothelial cells and nonkeratinizing epithelia. *Cell.* 31:693–703.

Yoshikawa, K., Y. Katagata, and S. Kondo. 1995. Relative amounts of keratin 17 are higher than those of keratin 16 in hair-follicle-derived tumors in comparison with nonfollicular epithelia skin tumors. *J. Invest. Dermatol.* 104: 396–400.